TABLE OF CONTENTS

CHAPTER		PAGE	
I.	INTRODUCTION	1	1/A11
II.	THE MODEL.....	4	1/A14
	1. The Equations of Motion.....	4	1/A11
	2. Bode Plots.....	6	1/B2
	3. Spectra of Wind Fields.....	17	1/B13
III.	AIRCRAFT APPROACH SIMULATIONS.....	20	1/C2
	1. Theory.....	20	1/C2
	2. Aircraft Simulations Using Real Data.....	23	1/C5
	3. An Example: JFK Crash, 1975.....	35	1/D3
IV.	CONCLUSIONS.....	48	1/E2
	REFERENCES.....	52	1/E6

Item 830-H-14
NAS1.26:3207
JAN 7 1980
COMPLETED

NASA Contractor Report 3207

ORIGINAL

Jet Transport Performance in Thunderstorm Wind Shear Conditions

John McCarthy, Edward F. Blick,
and Randall R. Bensch

CONTRACT NAS8-31377
DECEMBER 1979

NASA

63

NASA Contractor Report 3207

Jet Transport Performance in Thunderstorm Wind Shear Conditions

John McCarthy, Edward F. Blick,
and Randall R. Bensch
The University of Oklahoma
Norman, Oklahoma

Prepared for
Marshall Space Flight Center
under Contract NAS8-31377

National Aeronautics
and Space Administration

Scientific and Technical
Information Branch

1979

9.

This document, prepared under the sponsorship of the National Aeronautics and Space Administration, is disseminated in the interest of information exchanges. It does not necessarily represent the views, technical approaches, or conclusions of NASA or any of its officials. The United States Government assumes no liability for its contents or the use thereof.

AUTHORS' ACKNOWLEDGEMENTS

The work reported herein was supported by the National Aeronautics and Space Administration, Marshall Space Flight Center, Space Sciences Laboratory, Atmospheric Sciences Division, under contract number NAS8-31377.

The authors wish to thank Mr. John H. Enders of the Aviation Safety Technology Branch, Office of Aeronautics and Space Technology (OAST), NASA Headquarters, Washington, D. C., for his support of this research. We greatly appreciate the support of Mr. Dennis Camp, of the Marshall Space Flight Center, our project scientific monitor. Helpful discussions with Dr. Walter Frost, of the University of Tennessee Space Institute were important to this work.

The continuing support of the National Severe Storms Laboratory, Norman, Oklahoma, was vital to this work. Special thanks go to Dr. Edwin Kessler, Director, Dr. Richard Doviak, Dr. Ron Alberty, Mr. Stephan Nelson, and Mr. Jean T. Lee.

Aircraft data were provided by the Research Aviation Facility, National Center for Atmospheric Research, (NCAR), funded by the National Science Foundation, to whom we are grateful. The availability of NCAR aircraft data was due to NSF support for basic thunderstorm research, under NSF ATM74-0340ba02.

TABLE OF CONTENTS

CHAPTER		PAGE
I.	INTRODUCTION	1
II.	THE MODEL	4
	1. The Equations of Motion	4
	2. Bode Plots	6
	3. Spectra of Wind Fields	17
III.	AIRCRAFT APPROACH SIMULATIONS	20
	1. Theory	20
	2. Aircraft Simulations Using Real Data	23
	3. An Example: JFK Crash, 1975	35
IV.	CONCLUSIONS	48
	REFERENCES	52

LIST OF FIGURES

FIGURE		PAGE
1.	Wind gust Bode plots for Boeing 727 class airplane	9
2.	Response of Boeing 727 class airplane to (a) half sine wave tailwind gust and (b) elevator step input during landing	13
3.	Elevator angle Bode plots for Boeing 727 class airplane	16
4.	RMS altitude and velocity deviations of a Boeing 727 class airplane to continuous one $m \cdot sec^{-1}$ horizontal or vertical sine wave winds	18
5.	RMS altitude and velocity deviations of a Boeing 727 class airplane to horizontal wind shears	21
6.	RMS altitude and velocity deviations of a Boeing 727 class airplane to vertical wind shears	22
7.	Fixed-stick model simulation using NCAR aircraft data for 13 June 75 at 140230 CST	25
8.	Fixed-stick model simulation using NCAR aircraft data for 13 June 1975 at 142815 CST	26
9.	The square of the least-squares correlation coefficient (variance explained) plotted against frequency, (a) for 13 June 75, and (b) for 19 May 77	30
10.	Scattergrams relating $\Delta u'$ to ARWS function, expressed in dB, for (a) 13 June 75, and for (b) 19 May 77	32
11.	Sample simulation using KTVY tower data	33
12.	Another KTVY tower sample simulation	34

FIGURE PAGE

13. The square of the least-squares correlation coefficient (variance explained) plotted against frequency for eighty tower data simulations..... 36

14. Scattergrams relating Δu' to ARWS function, expressed in dB, for tower data..... 37

15. Longitudinal and vertical environment winds encountered by Eastern Flight 66..... 40

16. Model output for Eastern Flight 66 simulation..... 41

17. The estimated path of Eastern Flight 66, after Fujita and Caracena (1977)..... 47

NOMENCLATURE

C_D	drag coefficient (unitless)
C_L	lift coefficient (unitless)
h	aircraft altitude (m)
h_n	equilibrium aircraft altitude along a -3 deg glide slope (m)
$\Delta h'$	root-mean-square value of altitude deviation from -3 deg glide slope (m)
IAS	indicated airspeed ($m \cdot sec^{-1}$)
I_{yy}	mass moment of inertia about lateral (y) axis ($Kg \cdot m^2$)
q	aircraft angular pitch velocity ($\dot{\theta}$) ($rad \cdot sec^{-1}$)
u,w	airspeed and vertical velocity perturbations ($m \cdot sec^{-1}$)
$\Delta u'$	root-mean-square value of airspeed deviation from U_1 ($m \cdot sec^{-1}$)
U_1	equilibrium speed ($m \cdot sec^{-1}$)
X_u, X_w, X_δ	stability derivatives $\partial X/\partial u$ (sec^{-1}), $\partial X/\partial w$ (sec^{-1}) and $\partial X/\partial \delta$ ($m \cdot sec^{-2} \cdot rad^{-1}$)
$Z_u, Z_w, Z_{\dot{w}}, Z_q, Z_\delta$	stability derivatives $\partial Z/\partial u$ (sec^{-1}), $\partial Z/\partial w$ (sec^{-1}), $\partial Z/\partial \dot{w}$ (unitless), $\partial Z/\partial q$ ($m \cdot sec^{-1}$) and $\partial Z/\partial \delta$ ($m \cdot sec-2 \cdot rad^{-1}$)
$M_u, M_w, M_{\dot{w}}, M_q, M_\delta$	stability derivatives $\partial M/\partial u$ ($m^{-1} \cdot sec^{-1}$), $\partial M/\partial w$ ($m^{-1} \cdot sec^{-1}$), $\partial M/\partial \dot{w}$ (m^{-1}), $\partial M/\partial q$ (sec^{-1}) and $\partial M/\partial \delta$ ($sec^{-2} rad^{-1}$)
s	Laplace tranform variable (sec^{-1})
S	wing area (m^2)
t	time (sec)

t_L	landing time from 500 meter altitude to ground (sec)
TAS	aircraft true airspeed ($m \cdot sec^{-1}$)
u_g	environment gust velocity -- longitudinal component (tailwind is positive) ($m \cdot sec^{-1}$)
W	aircraft weight (newtons)
w_g	environment gust velocity -- vertical component (downdraft is positive) ($m \cdot sec^{-1}$)
δ_E	elevator angle (positive down) (rad)
ζ_{ph}	phugoid damping factor (unitless)
ζ_{sp}	short period damping factor (unitless)
θ	aircraft flight path angle with horizon (positive in a climb) (deg)
θ_1	equilibrium glide angle (deg)
ρ	air density ($Kg \cdot m^{-3}$)
T	phugoid time constant (sec)
ω_{ph}	phugoid frequency ($rad \cdot sec^{-1}$ or Hz)
ω_{sp}	short period frequency ($rad \cdot sec^{-1}$ or Hz)

CHAPTER I

INTRODUCTION

During the last few years, much attention has been directed toward thunderstorm-related approach and departure accidents involving civil and military jet transports. Various investigations of these accidents attribute the cause to severe wind shear. In particular, National Transportation Safety Board-NTSB (1976a) cited such a cause for the tragic end to Eastern Airlines Flight 66, at JFK Airport in New York, on June 24, 1975. Fujita and Byers (1977) and Fujita and Caracena (1977) have examined this and other accidents, arriving at the so-called "downburst-spearhead echo" theory of accident cause.

There have been a number of other reports related to the aircraft wind shear problem. Pertinent additional NTSB reports are NTSB (1974, 1976b). Fundamental studies describing how an aircraft responds to fluctuations in the wind are few. The authors of this report have produced McCarthy and Blick (1976), McCarthy et al. (1978a, 1978b). Recently Frost and Crosby (1978) and Frost and Reddy (1978) also examine the relationship between wind shear and aircraft response.

All too often, wind shear is examined without relating the shear to aircraft response, as in Fujita and Caracena (1977). Basic response theory of aircraft is examined in

standard texts such as Roskam (1972) and McRuer et al. (1973), without relating it to real atmospheric winds. We describe a study where actual winds measured by aircraft, in the thunderstorm environment, are used as input to a numerical simulation of aircraft flight, to determine response. We have posed a number of questions regarding aircraft landing or taking off in the thunderstorm environment:

1. Can the real winds near the earth's surface, which might adversely affect flight, be obtained?
2. Can a numerical model be developed which can test real wind profiles to determine whether an approach will be dangerously deteriorated?
3. With an affirmative answer for questions 1 and 2, can we obtain a reasonable estimate of whether a particular aircraft will experience difficulty, knowing the aircraft-encountered winds?
4. Can a real-time detection and warning system be developed using the information acquired in the pursuit described above?

With certain limitations, and yet a few uncertainties, we believe all of the above questions are answered in the positive.

To answer (1), we were fortunate to obtain several hours of three-dimensional wind data, collected by a meteorologically instrumented Queen Air airplane, on loan from the

National Center for Atmospheric Research (NCAR), which was flown within 500 m of the surface in the Oklahoma thunderstorm environment. Additional wind data were obtained from the National Severe Storms Laboratory (NSSL) instrumented tall tower in Oklahoma City. Finally, subjective wind profiles were obtained for an examination of Eastern Flight 66 crash from NTSB (1976a), data apparently described in Fujita and Caracena (1977).

A relatively simple numerical model for aircraft response was developed using a standard set of aircraft equations of motion, to pursue question (2). The model concentrated on fixed-stick approaches, or in other words, no pilot control inputs were considered.

Once we obtained the wind data and the model, we conducted approximately one thousand simulations of aircraft response to wind shear conditions associated with thunderstorms, including a graphic simulation of Eastern Flight 66. It was possible to arrive at a parameter we called the Approach Deterioration Parameter (ADP), which can be used to determine quantitatively whether a particular airplane can safely approach in specific wind shear conditions.

Although our work to this point has not been used as a real-time wind shear detection and warning system, we believe that our technique makes such a system feasible. Plans are underway to test this contention.

CHAPTER II

THE MODEL

1. The Equations of Motion

The equations used in the present analysis are essentially the classical equations of dynamic stability available from the literature, after Roskam (1972) and McRuer et al. (1973), with certain refinements made to describe the specific system under consideration. The refinements to the classical equations include the addition of wind gust forces.

The aircraft trajectory model employed in this study was derived based on the following assumptions:

a) The earth is flat and nonrotating.

b) The acceleration of gravity, g, is constant ($9.81\ m \cdot sec^{-2}$).

c) Air density is constant ($1.225\ kg \cdot m^{-3}$).

d) The airframe is a rigid body.

e) The aircraft is constrained to motion in the vertical plane.

f) The aircraft has a symmetry plane (the x-z plane).

g) The mass of the aircraft is constant.

h) Once the aircraft is trimmed, its throttle setting and elevator deflection angle are not changed (fixed-stick assumption).

i) The aerodynamic stability derivatives are constant

within the altitude and Mach number range experienced in this investigation.

The longitudinal linear differential equations of motion referenced to stability axes can be expressed as

$$\dot{u} - X_u u - X_w w + g\theta\cos\theta_1 = X_{\delta}\delta_E - X_u u_g - X_w w_g \tag{1}$$

$$-Z_u u + \dot{w} - Z_w w - Z_{\dot{w}}\dot{w} - Z_q\dot{\theta} + g\theta\sin\theta_1 = Z_{\delta}\delta_E - Z_u u_g - Z_w w_g \tag{2}$$

$$\ddot{\theta} - M_u u - M_w w - M_{\dot{w}}\dot{w} - M_q\dot{\theta} = M_{\delta}\delta_E - M_u u_g - (M_{\dot{w}} - M_q/U_1)\dot{w}_g - M_w w_g \; . \tag{3}$$

The auxiliary relationship needed to convert the motion variable of Eqs. (1)-(3) into altitude is,

$$\ddot{h} = -\dot{w} + U_1\dot{\theta} \; . \tag{4}$$

We selected to model a medium-size jet transport airplane (Boeing 727 class) because of its high use frequency, and its involvement in the Eastern 66 thunderstorm-related crash.

Eqs. (1)-(4) can be integrated numerically by Runge-Kutta schemes to obtain time-history motion as the aircraft flies along the glide slope or they can be used to develop Bode plots showing the variation of altitude and velocity

amplitudes for input sine wave gusts (horizontal and vertical).

Table 1 contains a list of the airplane characteristics used in the simulation.

Table 1. BOEING 727 CLASS - Medium size jet transport characteristics in landing mode.

Mass of Airplane.....63,958 kg (141,000 lb)	
Mass Moment of Inertia, I_{yy}....6.1×10^6 kg·m^2 (4.5×10^6 slug·ft^2)	
Wing Area.....145 m^2 (1560 ft^2)	
Fowler Flaps δ_E.....down 30 deg	
Glide Angle, θ_i.....-3 deg	
Initial Velocity, U_i.....72 m·sec^{-1} (140 kt)	
$X_u = -0.04065$ sec^{-1}	$M_w = -7.04 \times 10^{-3}$ m^{-1}·sec^{-1}
$X_w = 0.0738$ sec^{-1}	$M_{\dot{w}} = 2.69 \times 10^{-4}$ m^{-1}
$Z_u = -0.27263$ sec^{-1}	$M_q = -0.3228$ sec^{-1}
$Z_w = -0.622$ sec^{-1}	$X_\delta = 0$
$Z_{\dot{w}} = -0.0257$	$Z_\delta = -2.675$ m·sec^{-2}·rad^{-1}
$Z_q = -2.44$ m·sec^{-1}	$M_\delta = -0.503$ sec^{-2}·rad^{-1}
	$M_u = 0$

2. Bode Plots

In order to obtain some insight into the effects of horizontal and vertical wind gusts on aircraft speed and altitude, Bode plots can be constructed from Eqs. (1)-(4) for h/u_g, h/w_g, u/u_g and u/w_g, where for example, u/u_g represents

the perturbation airspeed u response to a perturbation gust in the longitudinal component u_g (a u/u_g of 10.0 means, for example, that a 1 $m \cdot sec^{-1}$ longitudinal gust input gives an airspeed output response of 10 $m \cdot sec^{-1}$).

In order to obtain the Bode plots it is necessary to obtain the transfer functions by first taking the Laplace transform of Eqs. (1)-(4) and then solving for the ratios of the Laplace transform variable. When this is done, one obtains the following equations:

$$\frac{u}{w_g} = \frac{1}{D} \begin{vmatrix} -X_{\dot{w}} & -X_w & g\cos\theta_1 \\ -Z_{\dot{w}} & S(1-Z_{\dot{w}}) - Z_w & -(U_1+Z_q)S + g\sin\theta_1 \\ -[(M_{\dot{w}} - M_q/U_1)S + M_w] & -(M_{\dot{w}}S + M_w) & S^2 - M_qS \end{vmatrix} \quad (5)$$

$$\frac{h}{w_g} = -\frac{1}{DS} \begin{vmatrix} S-X_u & -X_w & q\cos\theta \\ -Z_u & -Z_w & -(U_1 + Z_q)S + g\sin\theta_1 \\ -M_u & -[(M_{\dot{w}} - M_q/V_1)S + M_w] & S^2 - M_qS \end{vmatrix}$$

$$+ \frac{U_1}{DS} \begin{vmatrix} s - X_u & -X_w & -X_w \\ -Z_u & S(1 - Z_{\dot{w}}) - Z_w & -Z_w \\ -M_u & -(M_{\dot{w}}S + M_w) & -[(M_{\dot{w}} - M_q/V_1)S + M_w] \end{vmatrix} \quad (6)$$

$$\frac{u}{u_g} = \frac{1}{D}\begin{vmatrix} -X_u & -X_w & g\cos\theta_1 \\ -Z_u & S(1-Z_{\dot{w}}) - Z_w & -(V_1+Z_q)S + g\sin\theta_1 \\ -M_u & -(M_{\dot{w}}S + M_w) & S^2 - M_qS \end{vmatrix} \tag{7}$$

$$\frac{h}{u_g} = -\frac{1}{DS}\begin{vmatrix} S-X_u & -X_u & g\cos\theta_1 \\ -Z_u & -Z_u & -(V_1+Z_q)S + g\sin\theta_1 \\ -M_u & -M_u & S^2 - M_qS \end{vmatrix}$$

$$+ \frac{U_1}{DS}\begin{vmatrix} S-X_u & -X_w & -X_u \\ -Z_u & S(1-Z_{\dot{w}}) - Z_w & -Z_u \\ -M_u & -(M_{\dot{w}}S + M_w) & -M_u \end{vmatrix} \tag{8}$$

where

$$D = \begin{vmatrix} S-X_a & -X_w & g\cos\theta_1 \\ -Z_u & S(1-Z_{\dot{w}}) - Z_w & -(V_1+Z_q)S + g\sin\theta_1 \\ -M_u & -(M_{\dot{w}}S + M_w) & S^2 - M_qS \end{vmatrix} \tag{9}$$

Now to obtain the Bode plots, S is replaced in Eqs.(5)-(8) by $i\omega$ (where i is the imaginary number $\sqrt{-1}$). These equations can now be manipulated to obtain the magnitude ratios of the variables and the phase angle between them. These relations are plotted in Fig. 1.

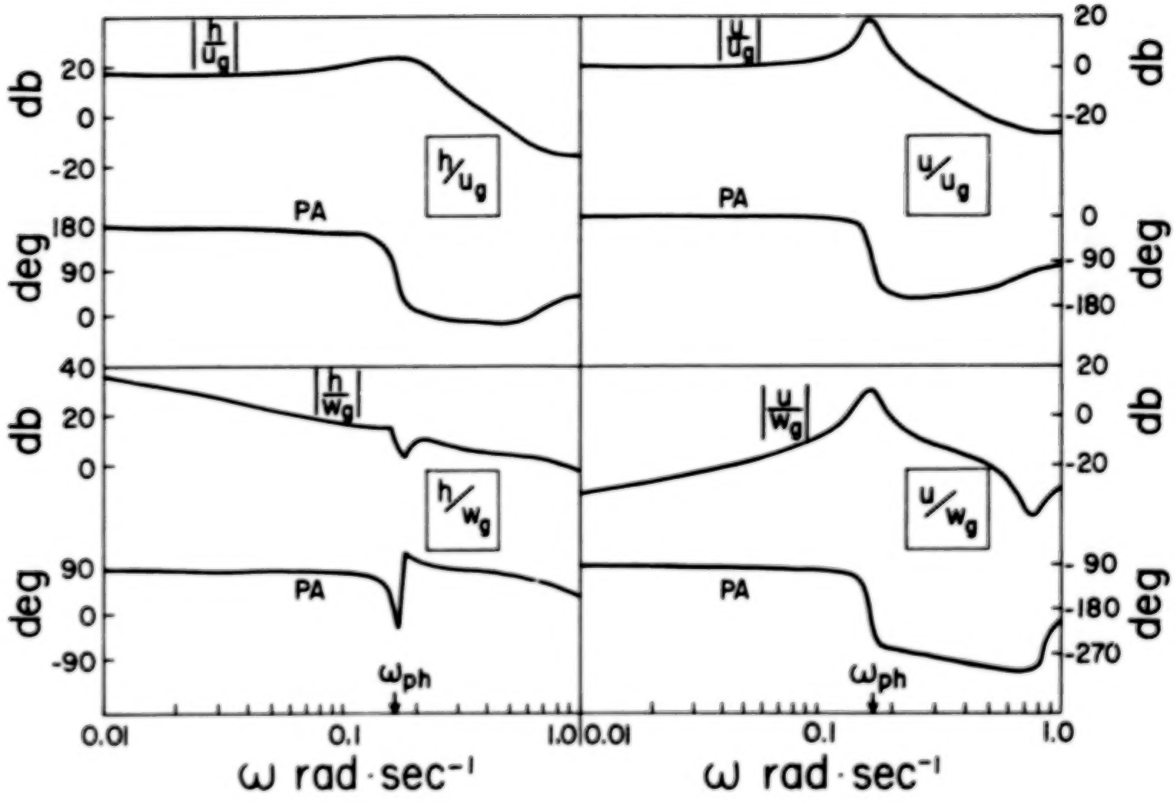

Fig. 1. Wind gust Bode plots for Boeing 727 class airplane.

It is interesting to note that a horizontal gust produces a large peak in the aircraft velocity perturbation u and a lesser peak in altitude perturbation h, at the aircraft angular phugoid frequency of 0.164 rad·sec^{-1}. The peak response for aircraft velocity perturbation is close to 20 db! This means that if a steady sinusoidal horizontal gust input of 2.1 m·sec^{-1} (4 kt) were encountered, the aircraft would respond with a sinusoidal velocity perturbation of approximately 21 m·sec^{-1} (40 kt)! This would mean that at one point in its cycles the aircraft would approach the stall speed of the aircraft, 51.5 m·sec^{-1} (100 kt), and a maximum speed of 92.7 m·sec^{-1} (180 kt) at another point during each sine wave cycle. Fig. 1 also indicates the aircraft perturbation altitude is also significantly affected by horizontal gusts when frequencies are at or below the phugoid frequency. Vertical sinusoidal gusts do not affect the aircraft velocity as much as the horizontal gusts. However, vertical sinusoidal gusts do produce larger changes in the airplane altitude then horizontal sinusoidal gusts at angular frequencies below 0.08 rad·sec^{-1}.

It is interesting to note that the height of the resonant peaks which occur at phugoid frequency in Fig. 1 can be related to several aircraft characteristics. When the characteristic equation of Eqs.(1)-(3) is determined (Eq. (9) set equal to zero), it can usually be written as the product

of two quadratic factors as shown by,

$$(s^2 + 2\zeta_{ph}\omega_{ph}s + \omega_{ph}^2)\cdot(s^2 + 2\zeta_{sp}\omega_{sp}s + \omega_{sp}^2) = 0 \ . \quad (10)$$

Each of the two quadratic factors contributes to the total Bode plots shown in Fig. 1. Usually the long period (phugoid) damping factor ζ_{ph} is much smaller than the short period damping factor ζ_{sp}. It can be easily shown that the resonant peak on a Bode plot due to a quadratic factor is $-20 \log_{10} (2\zeta)$. Hence for ζ less than 1.0 the resonant peak has a positive value. As ζ approaches zero, the peak becomes very large. It can be shown that for subsonic aircraft ζ_{ph} can usually be approximated by the following:

$$\zeta_{ph} \doteq \frac{1}{\sqrt{2}} \frac{C_D}{C_L} \ . \quad (11)$$

It can also be shown that the exponential phugoid time constant, T, is inversely proportional to $\zeta_{ph}\omega_{ph}$. Since ω_{ph} can be approximated by $1.4g/U_1$, then the phugoid mode time is approximated by

$$T \doteq \frac{U_1}{g} \frac{C_L}{C_D} \ . \quad (12)$$

Hence Eqs. (11) and (12) indicate that low values of ζ_{ph} and conversely large time constants which cause large excursions in aircraft perturbation speed (u) and altitude (h) are proportional to the lift-to-drag ratio of an airplane. Jet transports generally have large values of

lift-to-drag, even with their gear down in the landing mode. In addition, jet transports land at a high speed (compared to general aviation aircraft); hence the product of U_1 and C_L/C_D combine to produce a large value of the time constant in Eq. (12).

These factors would seem to suggest that light aircraft would not experience the same difficulty as a medium size jet transport when attempting to land in winds with large horizontal spectral components in the phugoid frequency range.

It is interesting to note that three minutes before Eastern Flight 66 (Boeing 727) crashed at New York's Kennedy Airport on June 24, 1975, a light aircraft (Beechcraft Baron) made a successful landing although it did experience a heavy sink rate and an airspeed drop of 10.3 $m \cdot sec^{-1}$ (20 kt), (from Fujita and Caracena, 1977). Reconstructions of the horizontal wind gusts from NTSB (1976a) showed the presence of a horizontal gust that was approximately one-half sine wave in length of angular frequency 0.16 $rad \cdot sec^{-1}$ (close to phugoid frequency of a Boeing 727) at an amplitude of approximately 13 $m \cdot sec^{-1}$! This case will be addressed in Chapter III.

That one does not need an endless string of horizontal wind gusts at or near the phugoid frequency to cause landing problems can be seen in Fig. 2a. The equations of motion (1)-(4) were solved for a Boeing 727 class airplane (Table 1) entering a -3 deg landing glide slope at 500 m altitude. The

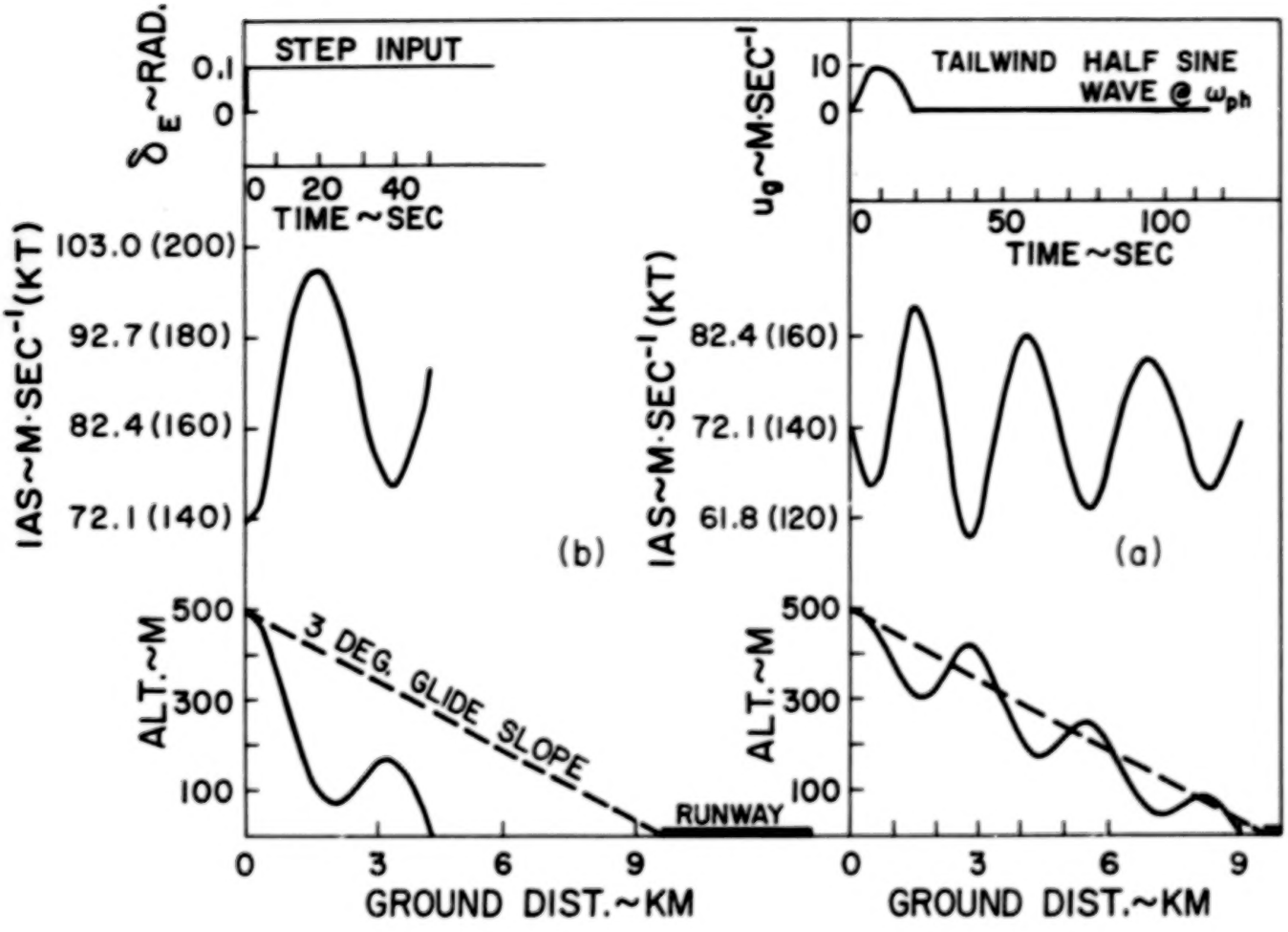

Fig. 2. Response of Boeing 727 class airplane to (a) half sine wave tailwind gust and (b) elevator step input during landing.

equations in stick-fixed mode were solved by the Continuous System Modeling Program (CSMP) method on the University of Oklahoma digital computer. A half sine wave tailwind of 10 $m \cdot sec^{-1}$ amplitude at the phugoid frequency was assumed to act on the airplane at an initial altitude of 500 m. The half sine horizontal tailwind lasted about 19 seconds. The resulting aircraft velocity deviations from an indicated airspeed of 72.1 $m \cdot sec^{-1}$ (140 kt) were as large as 13.9 $m \cdot sec^{-1}$ (27 kt). Even 76 sec after the gust had diminished to zero an airspeed deviation as large as 7.7 $m \cdot sec^{-1}$ (15 kt) was computed! The altitude deviations from the glide slope were as large as 100 m, 80 sec after the gust had diminished! The aircraft touched down 600 m short of the runway. So even a half sine wave gust near the phugoid frequency is extremely dangerous.

The problem for the pilot is how to control this roller coaster effect seen in Fig. 2. Suppose the pilot noticed the decrease in indicated air speed during the first five seconds (Fig. 2a) and decided to correct for this by a sudden deflection of the elevator 0.1 radian down, in order to pitch the nose down and pick up some speed. Fig. 2b shows that the airplane speed would not respond fully [IAS = 100.4 $m \cdot sec^{-1}$ (195 kt)] until a lag time of about 20 sec, but by now the airplane response to the one-half sine wave horizontal gust is 86.0 $m \cdot sec^{-1}$ (167 kt). Adding the two perturbation speeds

of (100.4-72.1) plus (86.0-72.1) one obtains an aircraft speed of 72.1 + 28.3 + 13.9 = 114.3 $m \cdot sec^{-1}$ (222 kt). Hence the pilot, in making what appeared to be an obvious correction to the elevator angle, actually made the system worse, i.e., he is making the aircraft unstable! Situations similar to the situation described in this paragraph may very well have occurred to aircraft in the past and caused the aircraft to crash during landing. It should be noted that one other obvious control the pilot has at his disposal is his throttle. However, this too could cause similar problems due to the long lag times required to "spool-up" the jet engines.

Bode plots (see Fig. 3) were also plotted for altitude response to elevator angle and aircraft perturbation velocity to elevator angle. Again peaks in amplitude plots are seen near the phugoid frequencies. Notice, at frequencies lower than the phugoid frequency, the phase angle for h/δ_E is about -180 deg (which is desirable since down elevator results in decreasing height). However, just above the phugoid frequency, h and δ_E are in phase which is undesirable (down elevator causes the airplane to climb). The u/δ_E Bode plot indicates that u and δ_E are in phase (desirable) at frequencies below phugoid frequency but are about -180 deg out of phase (undesirable) above the phugoid frequency. Fig. 3 then illustrates the problem a pilot has in adequately controlling a Boeing 727 class aircraft with the elevator in

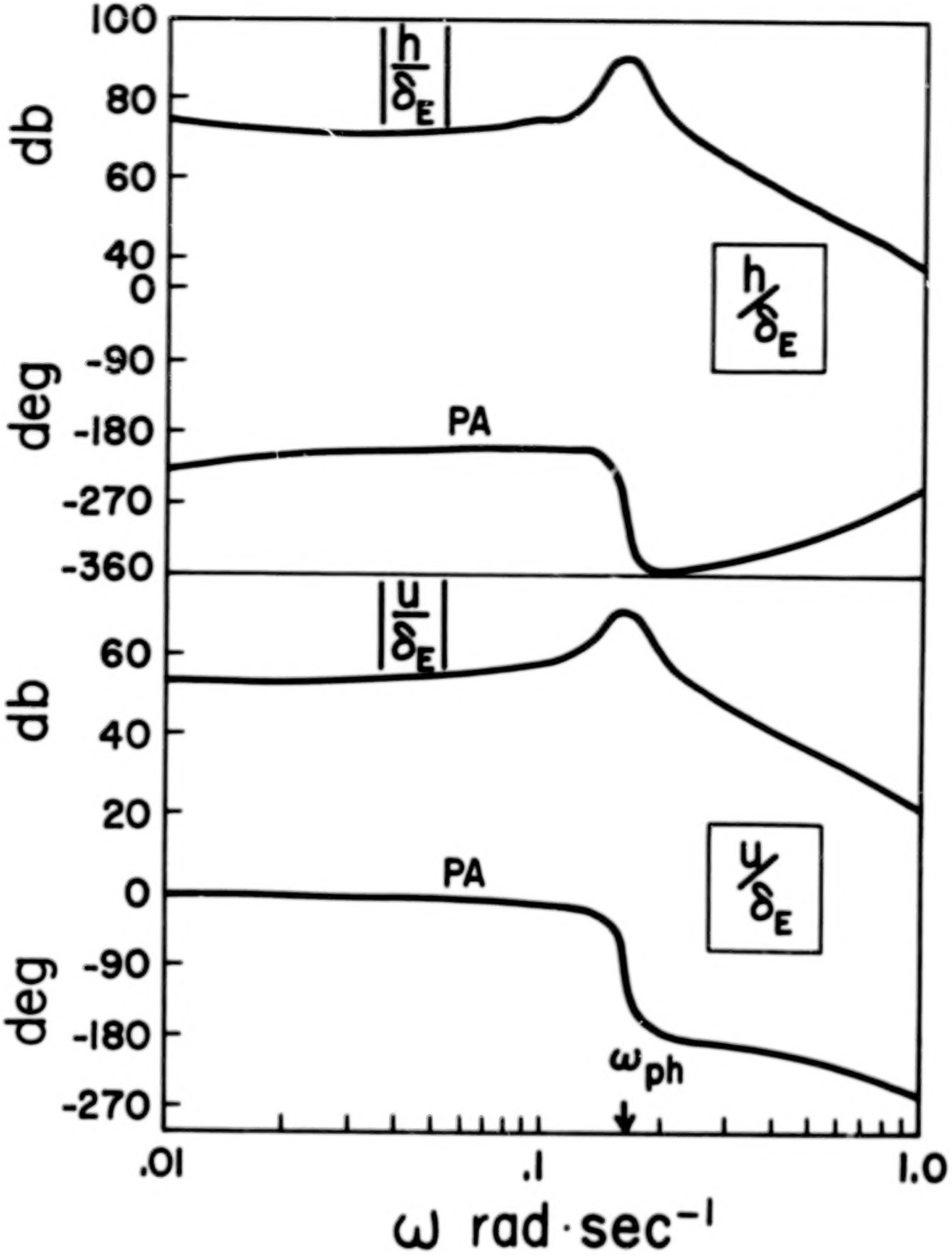

Fig. 3. Elevator angle Bode plots for Boeing 727 class airplane.

turbulent winds with strong spectral components in the phugoid frequency range.

3. Spectra of Wind Fields

A simple approximation to real wind fields is a set of sine waves. This is not realistic in terms of what happens in the atmosphere but by using such "pure tones" in the aircraft approach simulation model, discussed earlier, preliminary conclusions about aircraft performance can be obtained. For simulated Boeing 727 approaches from 500 m along a -3 deg glide slope, pure sine wave inputs, at various frequencies, have been used. Fig. 4 shows the root-mean-square values of airspeed and height deviations from the normal airspeed of 72.1 $m \cdot sec^{-1}$ (140 kt) and glide path due to a continuous 1.0 $m \cdot sec^{-1}$ amplitude input sine wave oscillation. Inputs in both the longitudinal (u_g) and vertical (w_g) components have been tested. It is obvious from the figure that maximum aircraft airspeed deviations occur for longitudinal inputs at the phugoid frequency. Vertical sinusoidal inputs do not affect the aircraft airspeed as much as the horizontal gusts. However, vertical inputs can cause much larger values of $\Delta h'$ than longitudinal inputs and the maximum value occurs at about one-sixth of the phugoid frequency.

Since pure sine waves seldom exist in the atmosphere, a better way to characterize the input wind fields is in terms of a variance or energy spectrum. This is given by energy

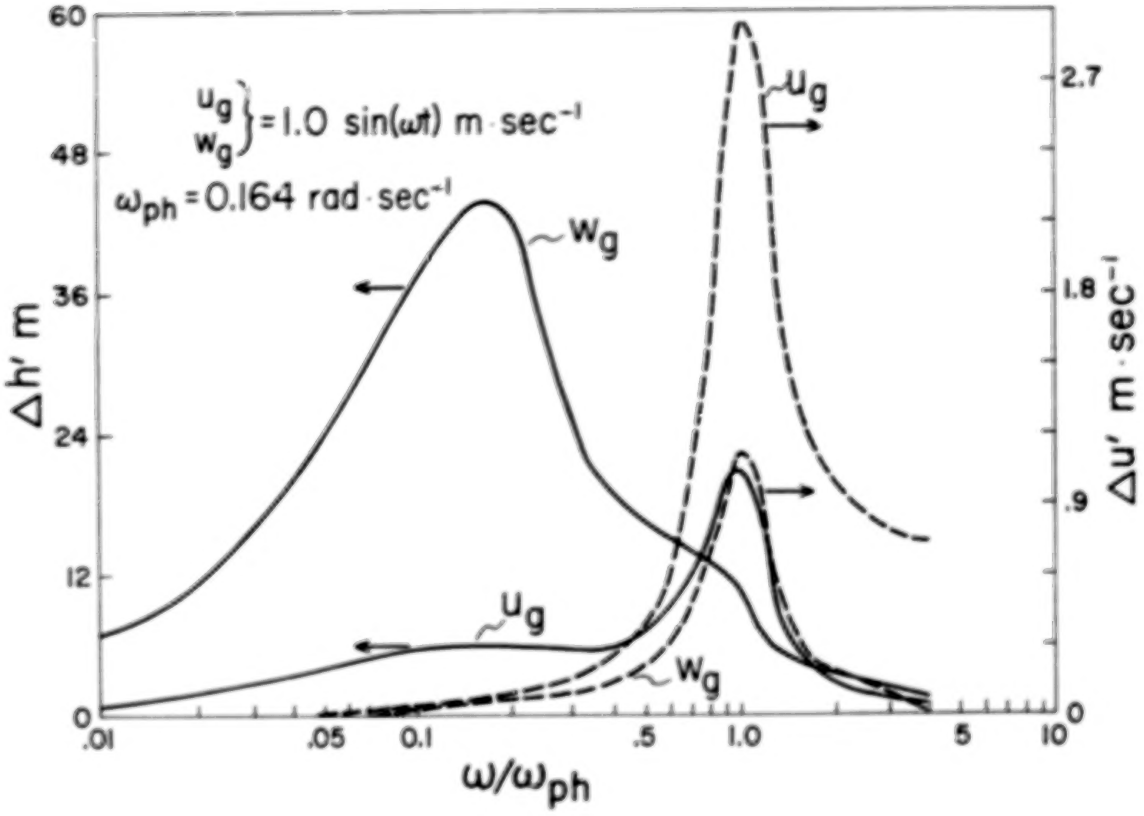

Fig. 4. RMS altitude and velocity deviations of a Boeing 727 class airplane to continuous one $m \cdot sec^{-1}$ horizontal or vertical sine wave winds during a landing from 500 m altitude to the ground.

density as a function of frequency. Since energy densities are used, a frequency interval is involved when actual energies (or associated amplitudes) are discussed.

There are several methods of obtaining variance spectra. We have chosen a technique described by Ulrych and Bishop (1975) as applied by Goerss and Koscielny (1977). This technique, referred to as the "maximum entropy" or auto-regressive modeling method, fits an optimum auto-regressive process to the given data to obtain energy density as a function of frequency. In all cases, one second data are used so that the frequency range is 0.0 to 0.5 Hz. We have used a frequency resolution of 0.002 Hz in finding the energy density, so the energy density is calculated for 251 frequencies.

Energy density spectra have been calculated for both the longitudinal and vertical wind components. For the longitudinal wind inputs, additional spectra have been produced. These spectra include not only the longitudinal wind input energy density, but also include an estimate of actual aircraft response; in particular, the airplane transfer function (u/u_g) is used. The energy density spectrum is multiplied by the transfer function squared to give a new energy spectrum, which we have called the Aircraft Response to Wind Spectrum (ARWS). The ARWS along with the longitudinal and vertical wind input spectra will be used in the discussions that follow.

CHAPTER III

AIRCRAFT APPROACH SIMULATIONS

1. Theory

At the heart of our research has been the modeling of aircraft performance to simulate aircraft approaches in various input wind fields. The basis of the model and the appropriate equations have been discussed in the previous chapter. The aircraft has been simulated to fly in a fixed-stick mode, in that no control or thrust changes are made during a simulated approach; in the model the aircraft remains perfectly trimmed for a -3 deg glide slope approach.

Fig. 5 presents solutions similar to the landing situation of Fig. 4 except instead of sinusoidal gusts, the Boeing 727 class airplane is experiencing horizontal wind shear of various magnitudes. There appears to be little significant difference in $\Delta h'$ and $\Delta u'$ between headwind or tailwind shears. Both types of shears cause the airplane to stall somewhere along its landing flight path for shear values in the vicinity of $\pm$ 4 $m \cdot sec^{-2}$.

Fig. 6 is the vertical wind shear equivalent of Fig. 5. For vertical downwinds which increase with time (positive values of w_g/t) the $\Delta h'$ values are about the same magnitude as the $\Delta h'$ values for u_g/t (Fig. 5). However, vertical wind shears ($\pm$ w_g/t) do not produce values of $\Delta u'$ as large as

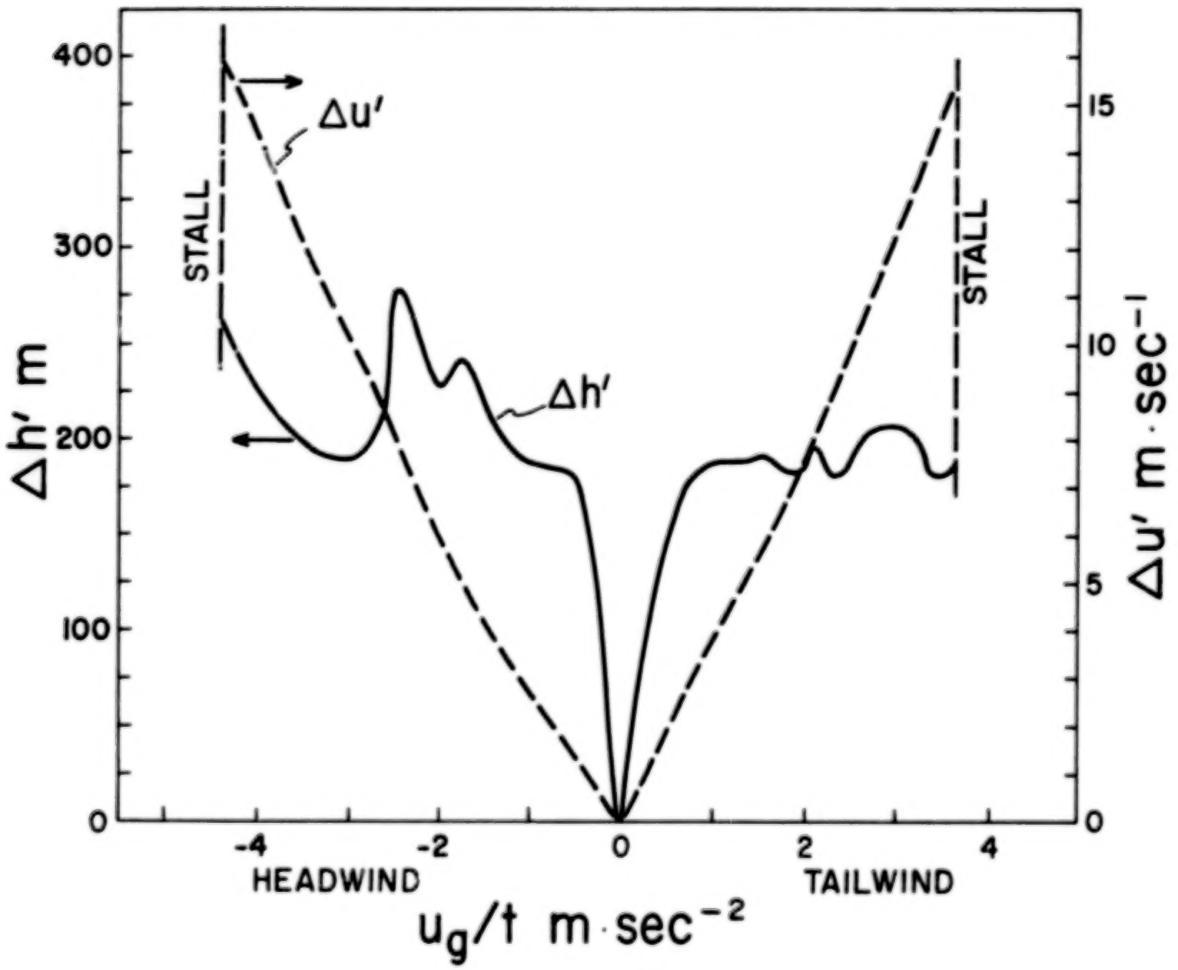

Fig. 5. RMS altitude and velocity deviations of a Boeing 727 class airplane to horizontal wind shears during a landing from 500 m altitude to the ground.

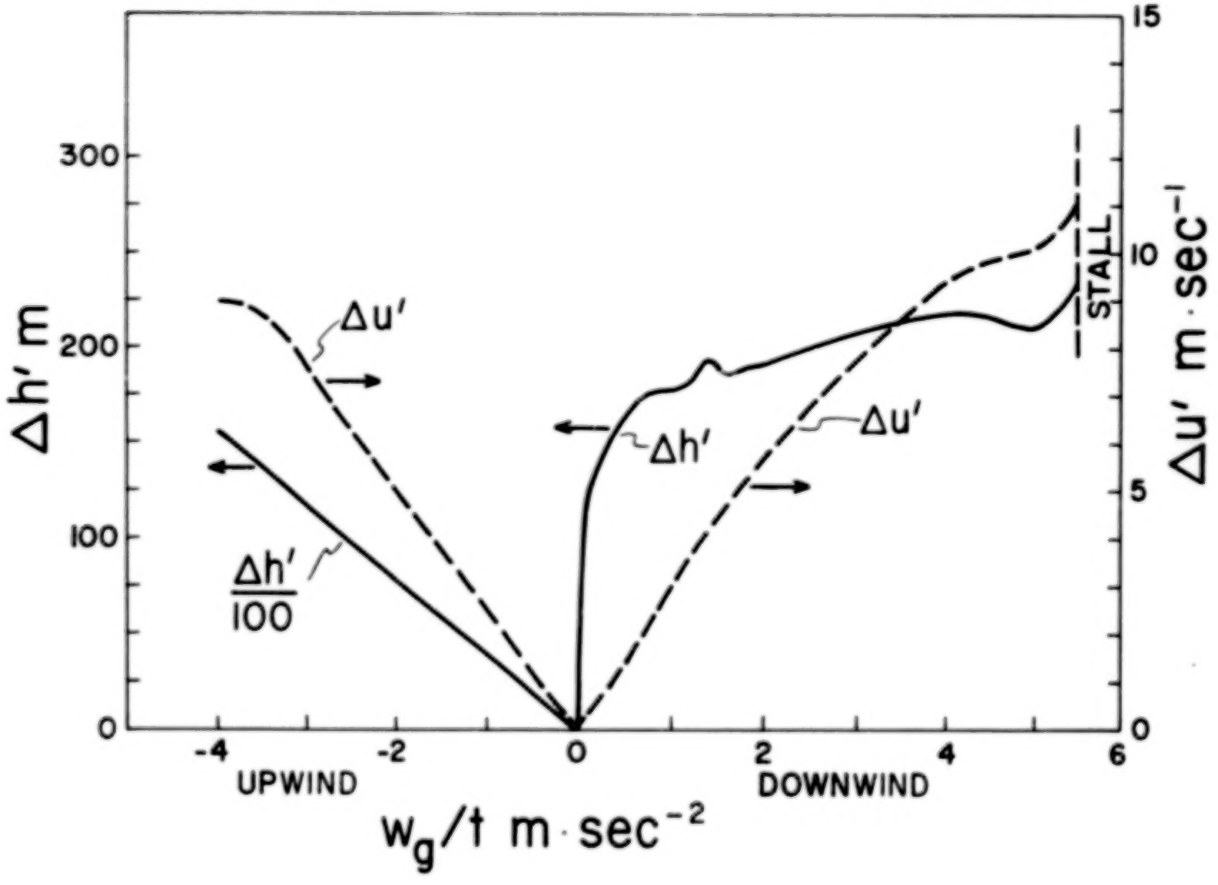

Fig. 6. RMS altitude and velocity deviations of a Boeing 727 class airplane to vertical wind shears during a landing from 500 m altitude to the ground.

those produced by $\pm u_g/t$ longitudinal wind shears. The large values of $\Delta h'$ produced by upwind shears are due to the fact that after a certain amount of time has passed, the vertical upwind is larger than the sink rate of the aircraft and the airplane never lands, but continues to climb. The $\Delta h'$ values for upwind shears have been computed for a time interval of 133 seconds (the normal landing time for descent from 500 m with no wind). All other $\Delta u'$ and $\Delta h'$ values shown in Figs. 4, 5 and 6 have been computed by the following formulae:

$$\Delta u' = \left[\frac{1}{t_L}\int_o^{t_L} u^2 dt\right]^{\frac{1}{2}} \tag{13}$$

$$\Delta h' = \left[\frac{1}{t_L}\int_o^{t_L} (h - h_n)^2 dt\right]^{\frac{1}{2}} . \tag{14}$$

2. Aircraft Simulations Using Real Data

The aircraft approach simulation model discussed in part III (1) has been used with actual measured winds. The two main sources for these winds have been 1) winds measured by research aircraft during flight, and 2) winds measured from a 444 meter-tall television tower.

(a) NCAR Aircraft Data

A prime source of data for winds near thunderstorms has been the National Center for Atmospheric Research (NCAR) Queen Air research aircraft. Such measurements were made, principally in the lowest 1 km of the atmosphere, on several days during the spring seasons of 1975 and 1977. These

aircraft are ideally suited for obtaining such data since they cruise at a speed close to that of the approach speed of a Boeing 727. The primary instrumentation system aboard the research aircraft is a gust probe wind measuring system coupled to an inertial navigation platform, providing 1.0 Hz sampling of the three-dimensional winds. Only the longitudinal and vertical wind components are used in this study.

As mentioned, the data are 1.0 Hz samples of longitudinal and vertical winds. The conventions of positive values for tailwind and downwind have been used. Data from two days have been used in the simulations. These days are 13 June 1975 (a day with tornadoes in Oklahoma) and 19 May 1977 (when the aircraft flew in the vicinity of a squall line and through the associated gust front). About two hours of data are available from each of the two flights. By initiating aircraft approach simulations at 15 sec steps into the data, a total of 480 simulations per flight have been produced.

Figs. 7 and 8 give details of two sample simulations from the 13 June 1975 data. Similar simulations have been produced for other times that day and for 19 May 1977. The heavy straight lines show the -3 deg glide slope centerline and the so-called "missed approach" of -3 deg $\pm$ 0.7 deg. The sequence of numbers "1" gives the actual aircraft position for each 2 sec from the initial time shown. The data panels give 1.0 Hz values of u_g, w_g, true airspeed (TAS),

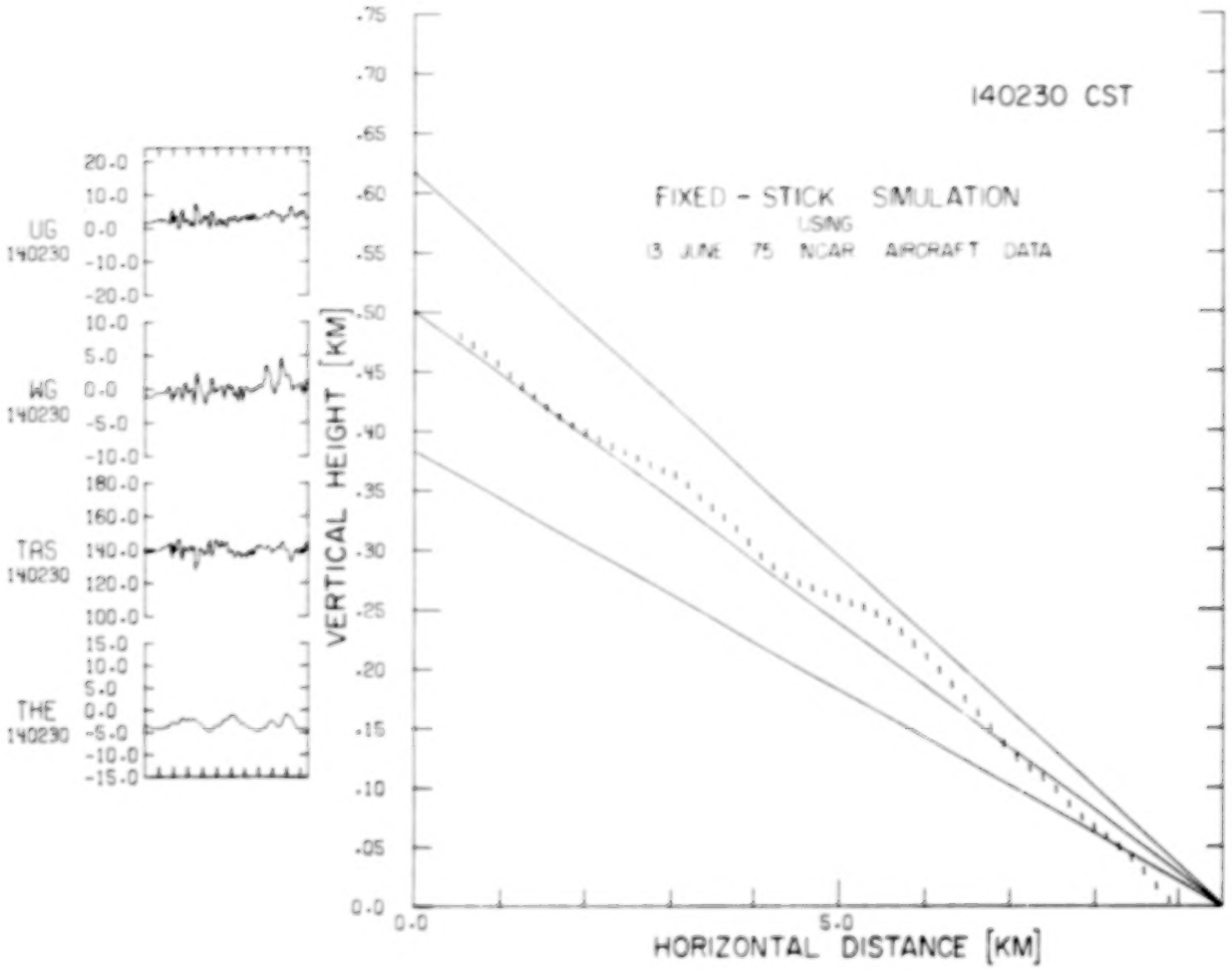

Fig. 7. Fixed-stick model simulation using NCAR aircraft data for 13 June 1975 at 140230 CST. Data panels show u_g, w_g input and TAS and θ output, with time increasing to the right, with each division 10 sec. Larger panel shows aircraft position with respect to -3 deg $\pm$ 0.7 deg glide slope to nominal touchdown at lower right. Case demonstrates that seemingly turbulent input results in relatively good approach.

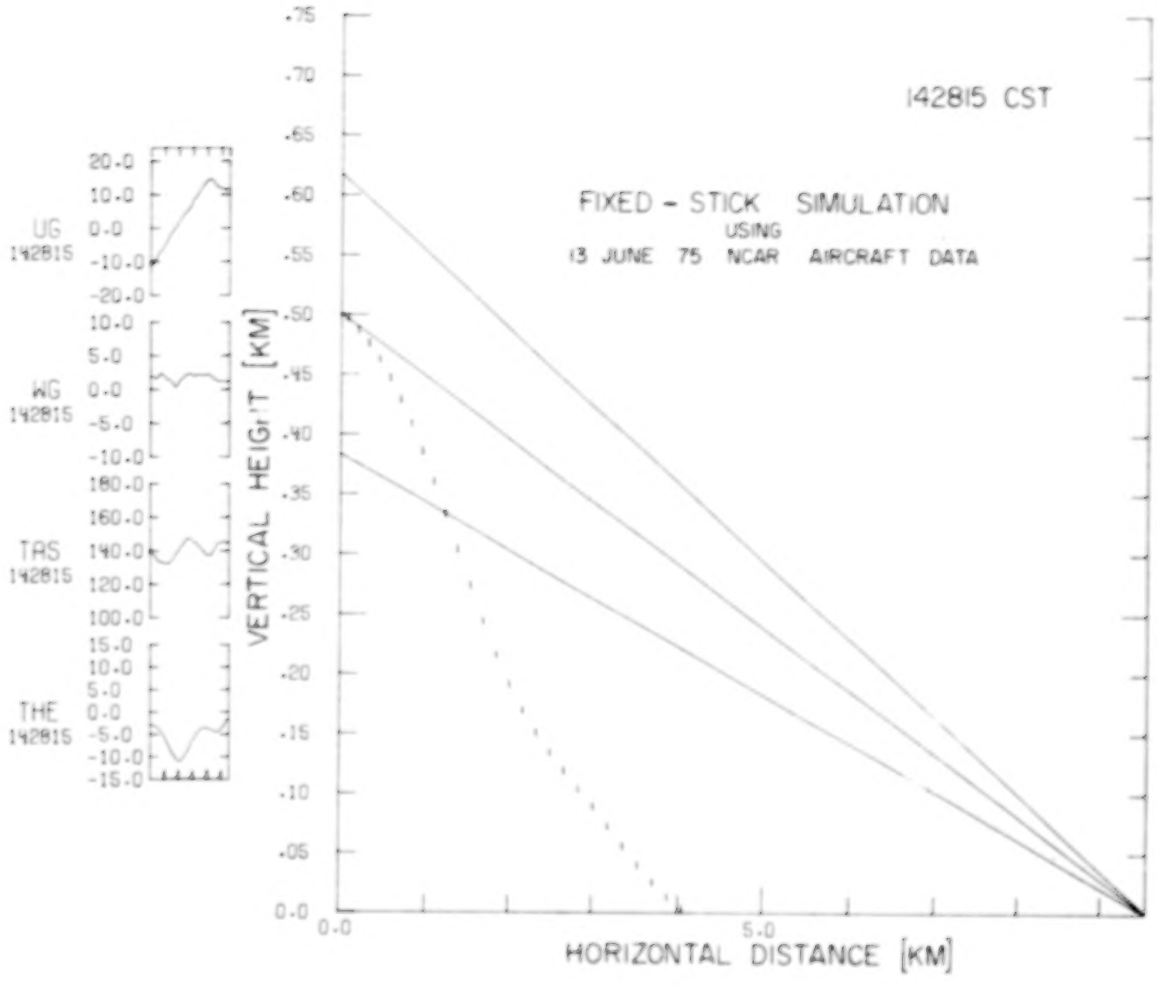

Fig. 8. Same as Fig. 7, for starting time of 142815 CST. Demonstrates non-turbulent but high shear input results in poor approach.

and pitch angle (θ). The first case is interesting in that the approach is "quite good" since departures from nominal [TAS = 72.1 $m \cdot sec^{-1}$ (140 kt) and "on the beam"] are small, even though the input winds appear to be turbulent. The second case (Fig. 8) demonstrates a situation where the departure from the glide slope is extreme, while turbulent velocity deviations are relatively minor.

To better quantify these "departures", variables $\Delta u'$ and $\Delta h'$, as defined by Eqs. (13) and (14), were calculated for the 480 simulations for each day. Each quantity $\Delta u'$ and $\Delta h'$, can be considered as Approach Deterioration Parameter (ADP) under the assumption that significant velocity deviations from the nominal true airspeed and height deviations from the glide path represent deterioration of the approach. Table 2 gives the appropriate values for the example cases.

Table 2. Approach Deterioration Parameters and shear values for the two examples given in Figs. 7 and 8, 13 June 1975.

Time	$\Delta u'$ $m \cdot sec^{-1}$	$\Delta h'$ m	$(\overline{u_g/t})_1$ $m \cdot sec^{-2}$	$(\overline{u_g/t})_{30}$ $m \cdot sec^{-2}$	$(\overline{w_g/t})_1$ $m \cdot sec^{-2}$	$(\overline{w_g/t})_{30}$ $m \cdot sec^{-2}$
140230	1.6	14.8	1.06	0.078	0.63	0.040
142815	2.5	193.7	0.26	0.176	0.09	0.017

An attempt has been made to correlate shear values for u_g and w_g, to the values of ADP. Table 3 gives the least-squares linear regression correlation coefficients for four shear values. The subscripts indicate the number of seconds

for which the mean shear is calculated. Clearly for the $\Delta u'$ parameter, reasonably high correlations occur, while for $\Delta h'$ no significant relationship appears, especially for the 13 June 1975 data. The fact that $\Delta u'$ is highly correlated and $\Delta h'$ is less highly correlated can be understood by examining the relationship between $\Delta u'$, $\Delta h'$ and the shears as seen in Figs. 5 and 6. $\Delta u'$ is seen to plot as very nearly straight lines in Figs. 5 and 6 while $\Delta h'$ does not, and is, in fact, a rather complex non-linear function.

Table 3. Least-squares linear correlation coefficients between indicated shears (independent variable) and two Approach Deterioration Parameters for 480 simulations (13 June 1975 data). Values for 19 May 1977 data are shown in parentheses.

Shear Values	$\Delta u'$ ($m \cdot sec^{-1}$)	$\Delta h'$ (m)
	(0.63)	(0.47)
$(\overline{u_g/t})_1$	0.68	0.09
	(0.50)	(0.62)
$(\overline{u_g/t})_{30}$	0.35	0.30
	(0.47)	(0.37)
$(\overline{w_g/t})_1$	0.69	0.10
	(0.46)	(0.43)
$(\overline{w_g/t})_{30}$	0.70	0.01

Variance spectra, as described in part II (3) have been found for each of the first 470 input data sets for the two

research days (13 June 1975 and 19 May 1977). Each spectrum is calculated at 251 frequencies from 0.0 to 0.5 Hz. For frequencies at regular intervals, a least-squares fit is made correlating 470 pairs: the energy density at a given frequency and the value of $\Delta u'$ for that simulation. A first order correlation coefficient is calculated for each frequency. Fig. 9 contains plots of the square of the correlation coefficient (positive correlation) against frequency for the two days. Two curves are shown in each plot, one for u_g and one for w_g. Correlations have been run for the special case of ω_{ph} (.026 Hz) and are shown with the small x's.

These results support the ideas presented in Fig. 4. That is, $\Delta u'$ is greater when a large amount of energy is present in the u_g field centered about the phugoid frequency. In other words, there is a strong linear relationship between $\Delta u'$ and high energy density at ω_{ph}, a relationship which breaks down at frequencies significantly different from ω_{ph}. However, a similar correlation peak is not seen in the w_g field at ω_{ph}, nor, from Fig. 4, would it be particularly important for aircraft approach quality were it present. Clearly then, we can conclude that longitudinal wind gusts providing energy at the phugoid frequency may result in airspeed oscillations of a nature that would be difficult to control, and in fact may lead to stall, and otherwise disastrous results.

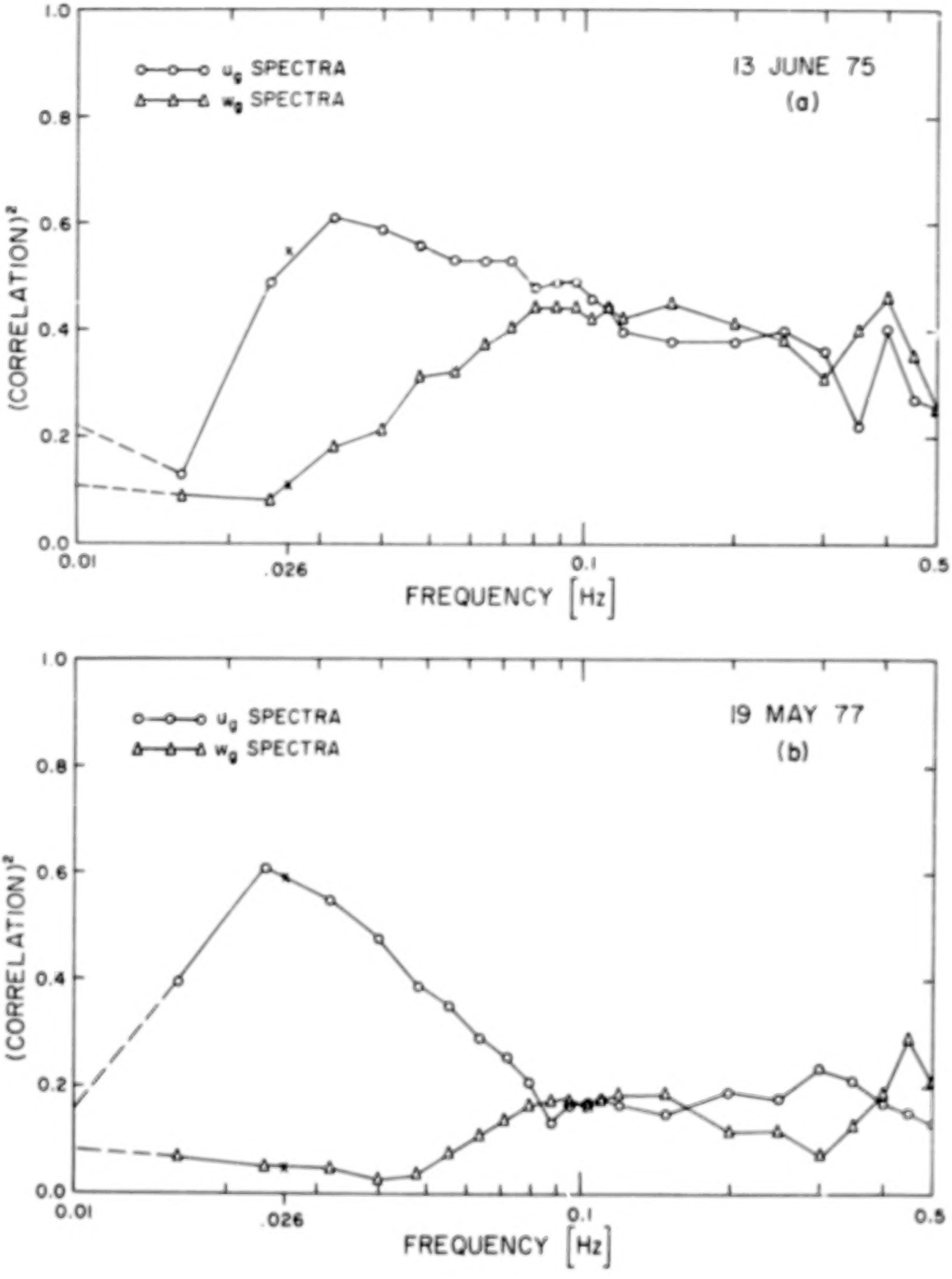

Fig. 9. The square of the least-squares correlation coefficient (variance explained) plotted against frequency for (a) 13 June 1975 and (b) 19 May 1977. See text for explanation.

The $\Delta u'$ values are plotted as functions of the peak value of the ARWS [discussed in part II (3)] in Fig. 10. Again both days are shown. The ARWS appears to be a better predictor for estimating approach quality. Close inspection of Fig. 10 shows that ambiguities remain, since a precise $\Delta u'$ cannot be predicted from a given ARWS. Instead, only a critical threshold can be seen, beyond which large values of $\Delta u'$ might occur. An unanswered question is what value of ARWS is critical? This question will be addressed in part III (3).

(b) KTVY Tower Data

Another source of data has been space-time adjusted fields of winds from the 444 meter instrumented KTVY-TV tower located in northern Oklahoma City, Oklahoma. Twenty thunderstorm influenced cases have been used to produce input winds for the simulation model. Approach wind conditions are obtained along approach paths in each direction through the two dimensional data fields. Also turbulence has been added by a numerical model of turbulence to create a second set of 40 input winds for simulations. Thus a total of 80 approach wind inputs are available for use in the Boeing 727 simulation model. Tower data were processed by use of a computer program developed by Frost et al. (1978).

Samples of these simulations are shown in Figs. 11 and 12. These show extreme cases of aircraft performance. Fig. 11 shows input winds with small scale turbulence but no large

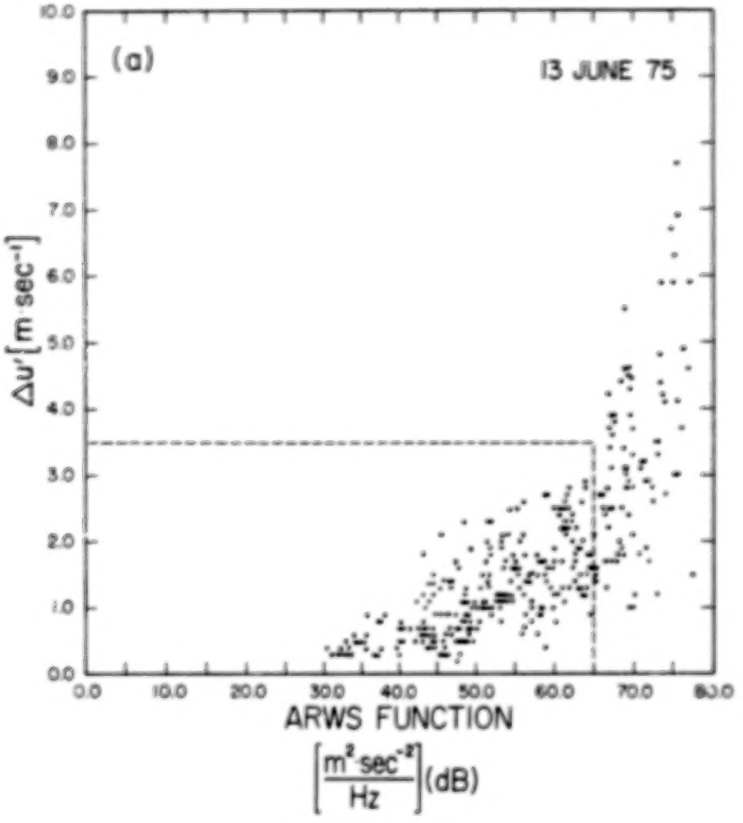

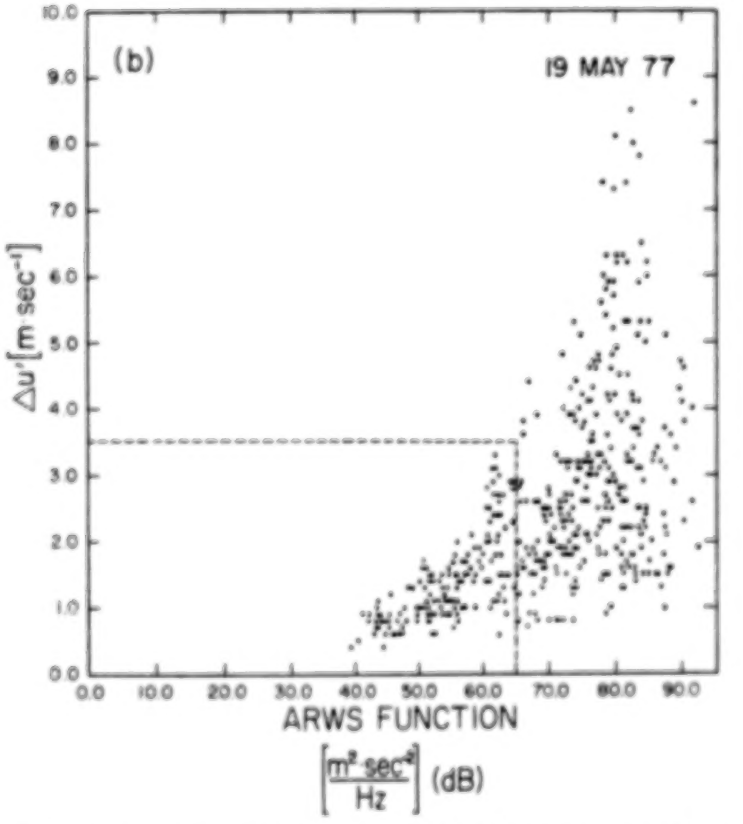

Fig. 10. Scattergrams relating Δu' to ARWS function, expressed in dB, for (a) 13 June 1975 and (b) 19 May 1977. JFK accident example shows a computed ARWS value of 65 $m^2 \cdot sec^{-2} \cdot Hz^{-1}$ predicts a Δu' RMS velocity departure of 3.5 $m \cdot sec^{-1}$.

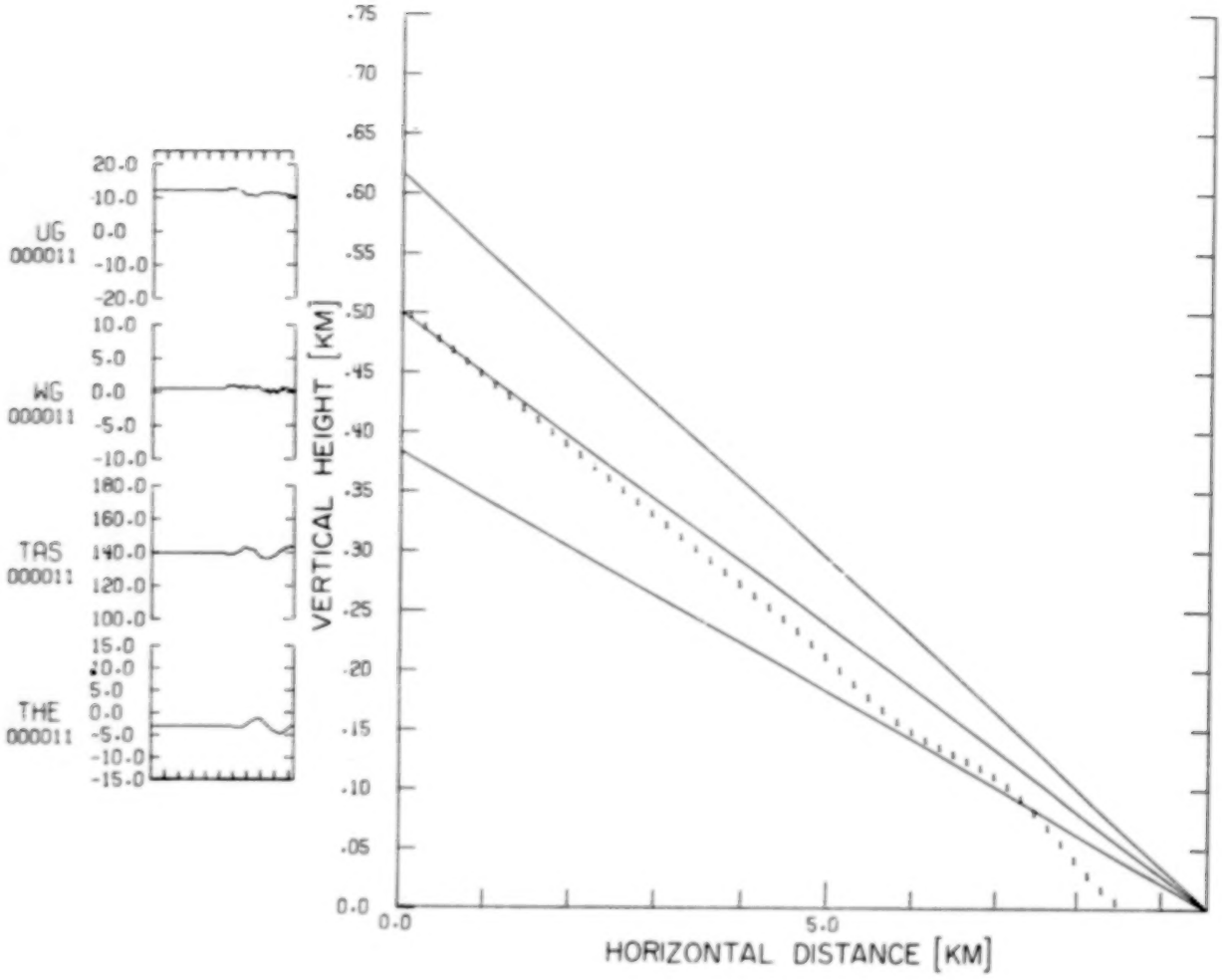

Fig. 11. Same as Fig. 7, for a sample simulation using tower data. Demonstrates small amplitude turbulence with a good approach.

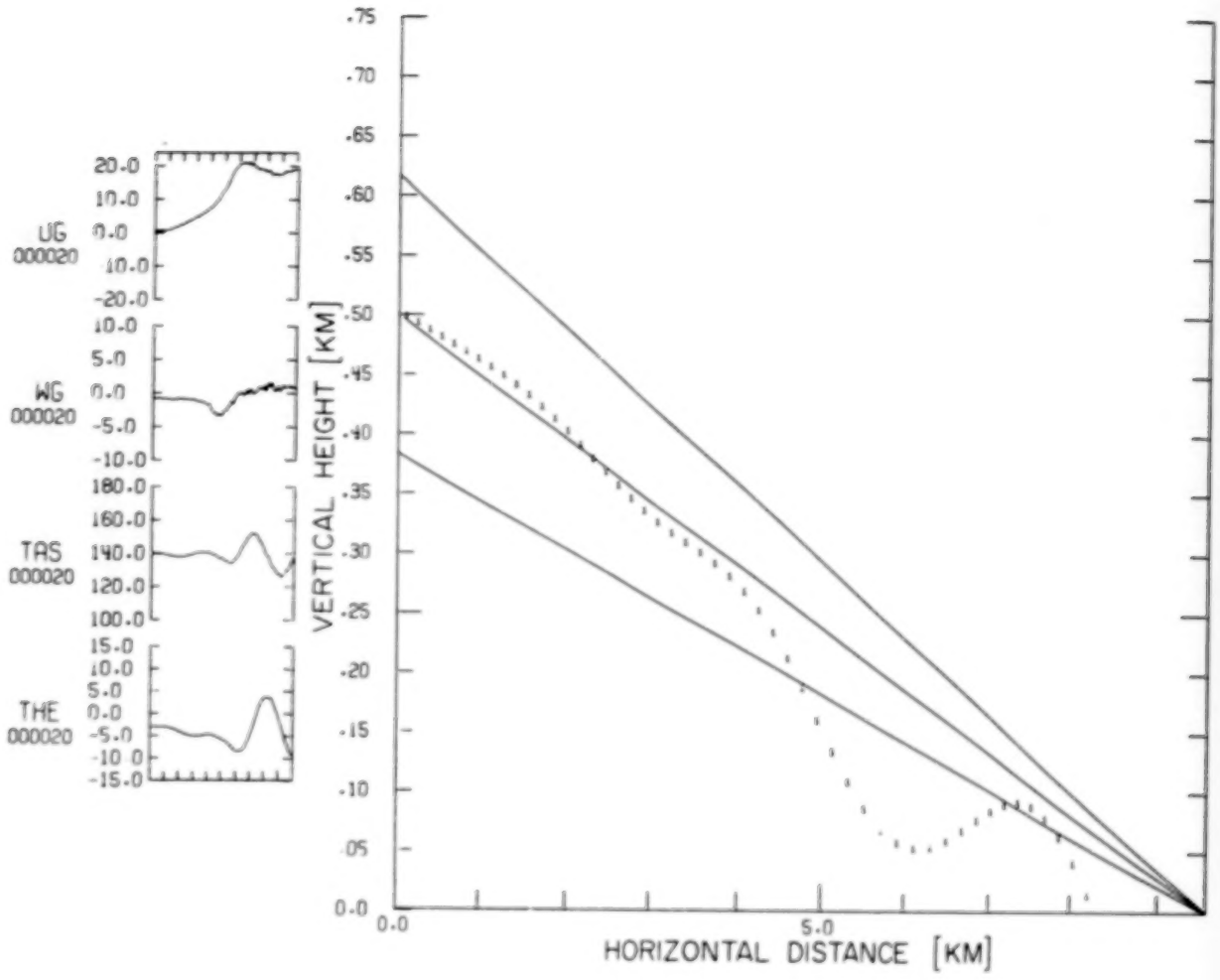

Fig. 12. Same as Fig. 7, for a sample simulation using tower data. Demonstrates wave-like input which results in a poor approach.

fluctuations over sustained time periods. The aircraft performance is good with only slight airspeed changes. The aircraft does drift somewhat below the glide slope due to the downdraft (positive w_g). In Fig. 12, a large change in u_g over a number of seconds produces rather large fluctuations in airspeed and aircraft height.

Fig. 13 is comparable to Fig. 9 except it is for the 80 tower wind cases. Notice that the results are different. The correlations are smaller and the peak for the u_g spectra, near the phugoid frequency, is not seen. The smaller sample size (80 vs. 470) may be a factor in these differences.

Fig. 14 includes scattergrams for $\Delta u'$ as a function of the peak value of ARWS. Three sets are included: 1) 40 cases of data with no turbulence added, 2) 40 cases with turbulence added, and 3) 80 cases consisting of the combination of both. The patterns are rather similar in each plot and agree with the larger sample shown in Fig. 10, and the conclusions reached in the discussion of Fig. 10 apply here as well.

3. An Example: JFK Crash, 1975

The tragic crash of Eastern Airlines Flight 66 at John F. Kennedy Airport on 24 June 1975 has focused the attention of aeronautical engineers and meteorologists on the problem of landing aircraft in thunderstorm related environments. The National Transportation Safety Board in NTSB (1976a) has stated that the probable cause of Eastern Airlines' Flight 66

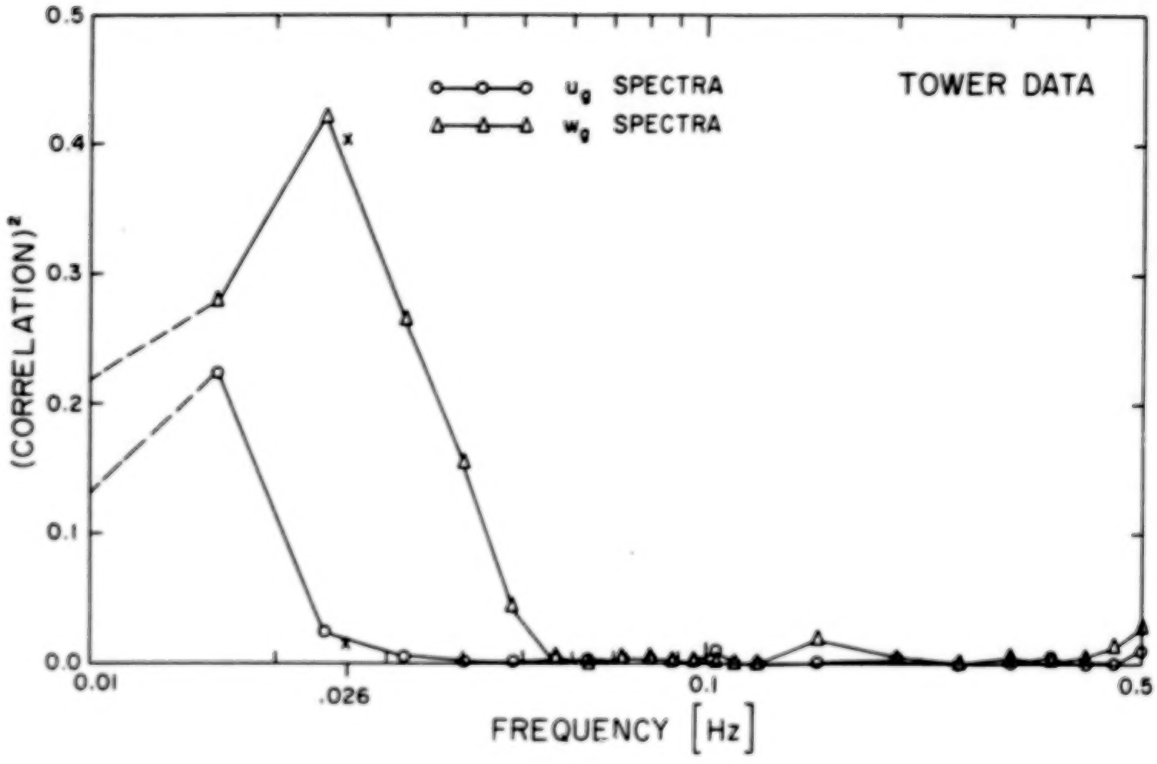

Fig. 13. Same as Fig. 9, for eighty tower data simulations.

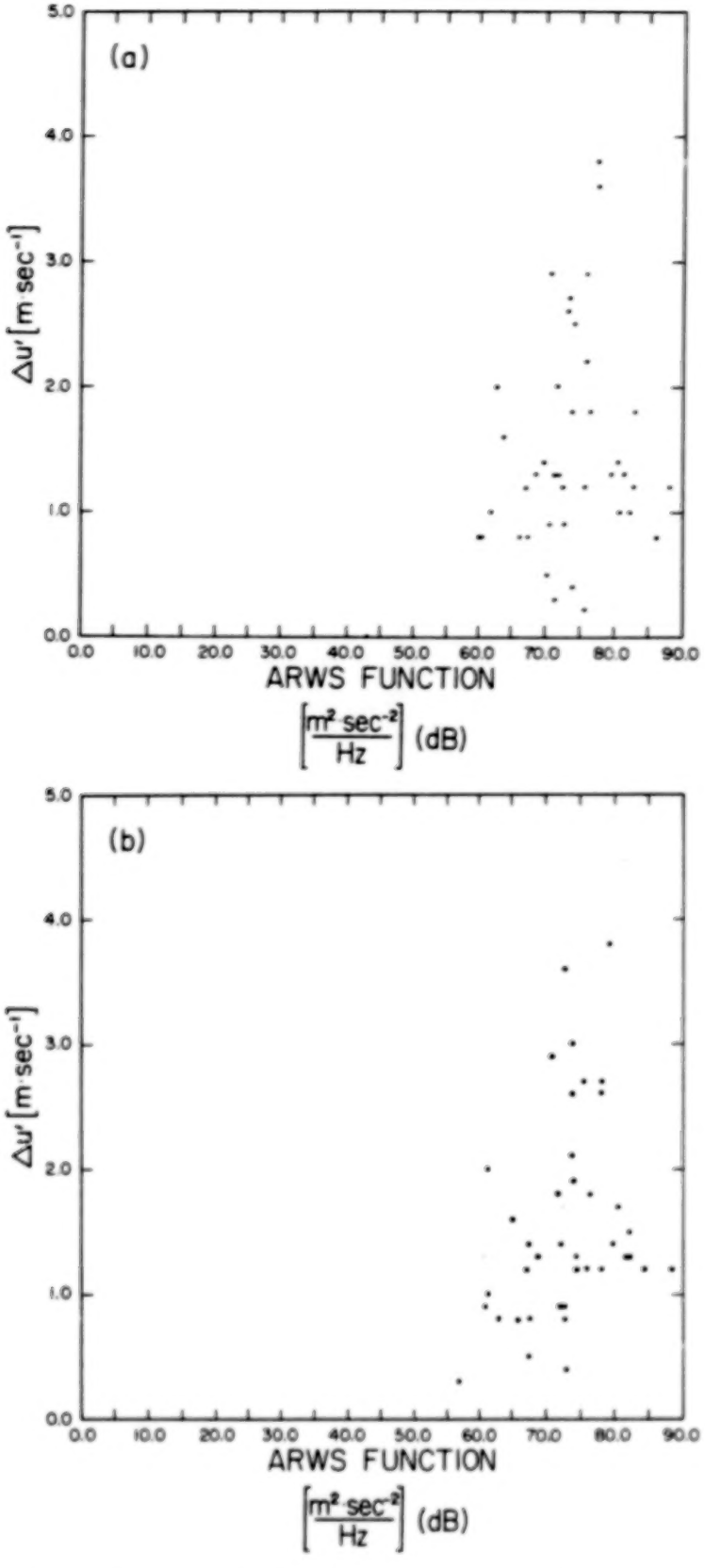

Fig. 14. Plots same as Fig. 10, for (a) tower data cases, (b) tower data cases with turbulence added and (c) both (continued on next page).

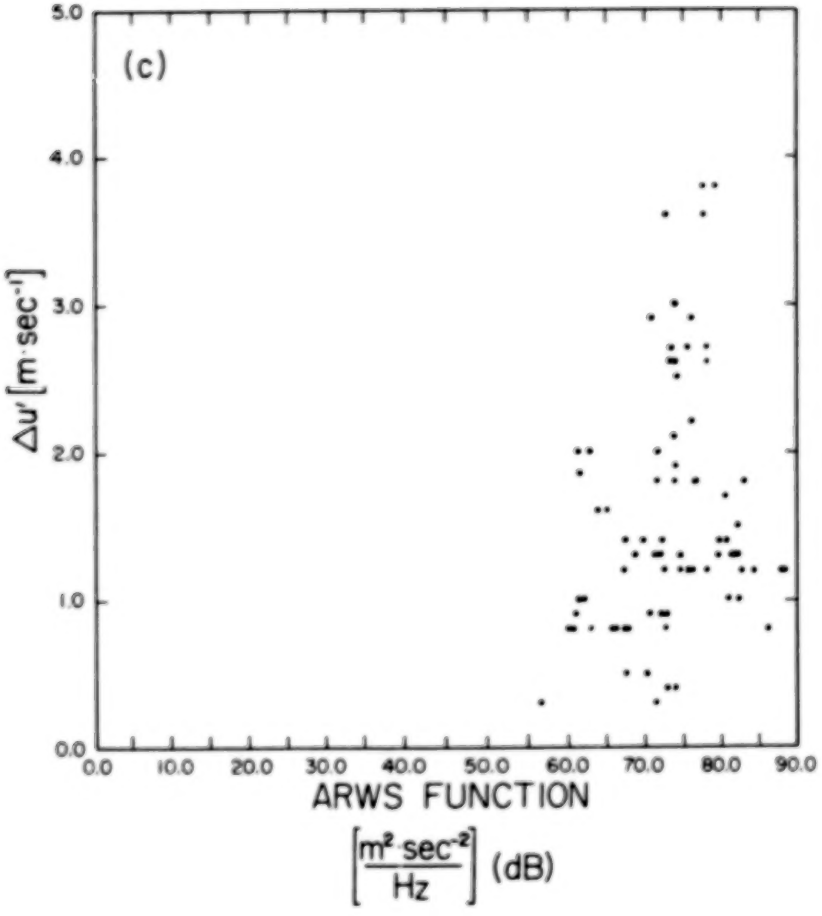

Fig. 14. Continued.

accident was "...an encounter with adverse winds associated with a very strong thunderstorm located astride the ILS localizer course which resulted in a high descent rate into non-frangible approach light towers."

We have examined the Eastern 66 crash using the Boeing 727 simulation model. Although data are sparse for the winds encountered by the aircraft, the relatively simple description of the winds found in NTSB (1976a) is used here. Fig. 15 gives the u_g and w_g wind components taken directly from the NTSB report (page 17), and placed on a simulated -3 deg glide slope approach. Fig. 16(a) gives the simulated position of the aircraft relative to the ILS corridor, while 16(b) gives the simulated true airspeed. Three cases have been run: u_g with $w_g = 0$, w_g with $u_g = 0$, and $u_g w_g$, all using the fixed-stick mode.

Several interesting observations can be made, related in particular to Fig. 4. When u_g is taken alone, input is an apparent one-half wave of period of approximately 19 sec, or a full wave of 38 sec; for such a wave the energy is concentrated at 0.026 Hz, precisely the phugoid frequency! We give computed values of ADP as a function of frequency, so comparisons to Fig. 4 might be made; such a comparison for the u_g case is quite good. The case of the w_g fluctuation must be considered in a little more d[illegible] In Fig. 15, we see more of a pure shear of -10.8 $m \cdot sec^{-1}$ over about 12 sec,

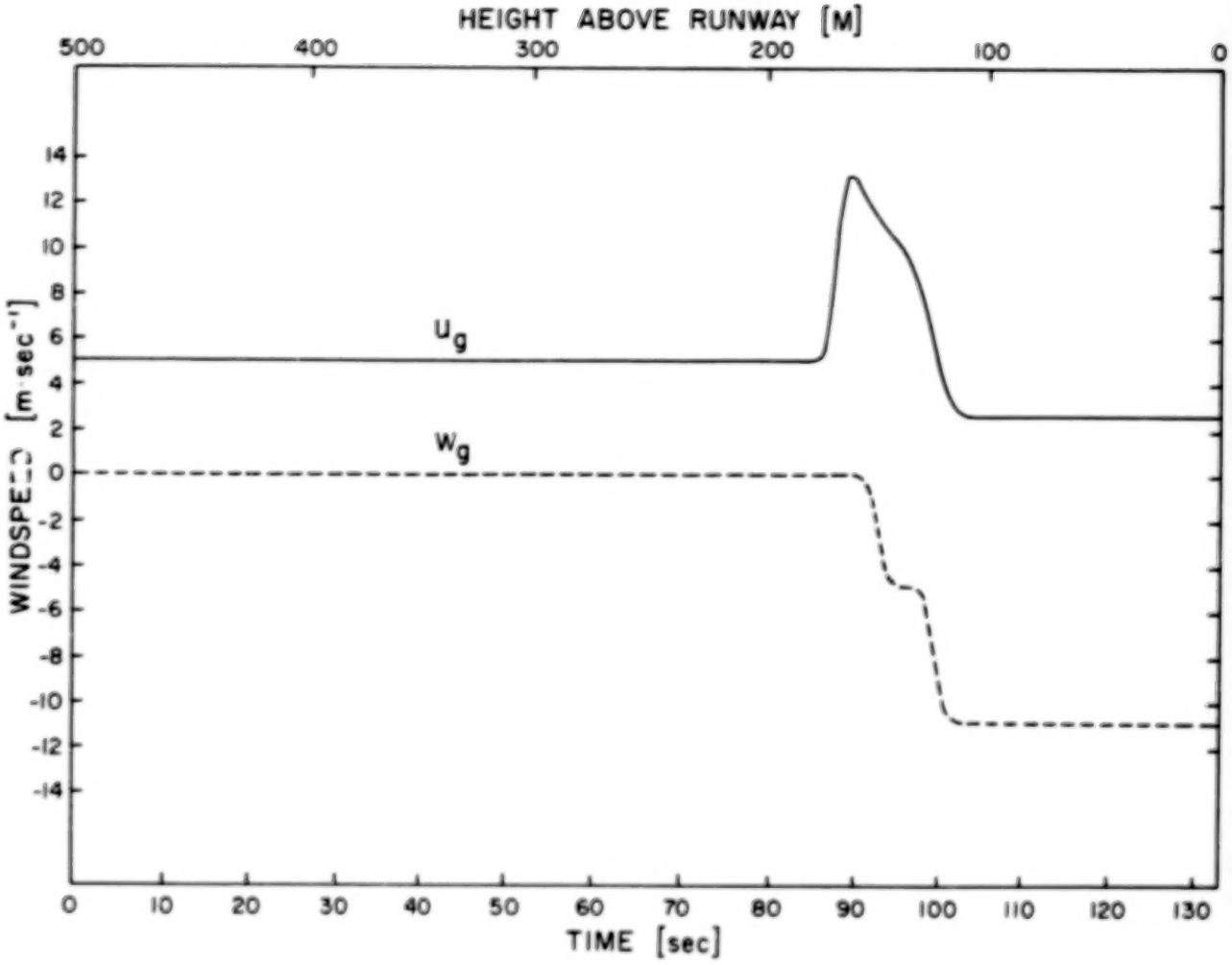

Fig. 15. Longitudinal and vertical environment winds encountered by Eastern Flight 66, as derived from NTSB (1976). Subjective smoothing was applied to the data; no turbulence fluctuations were added. A u_g headwind and a w_g updraft are positive.

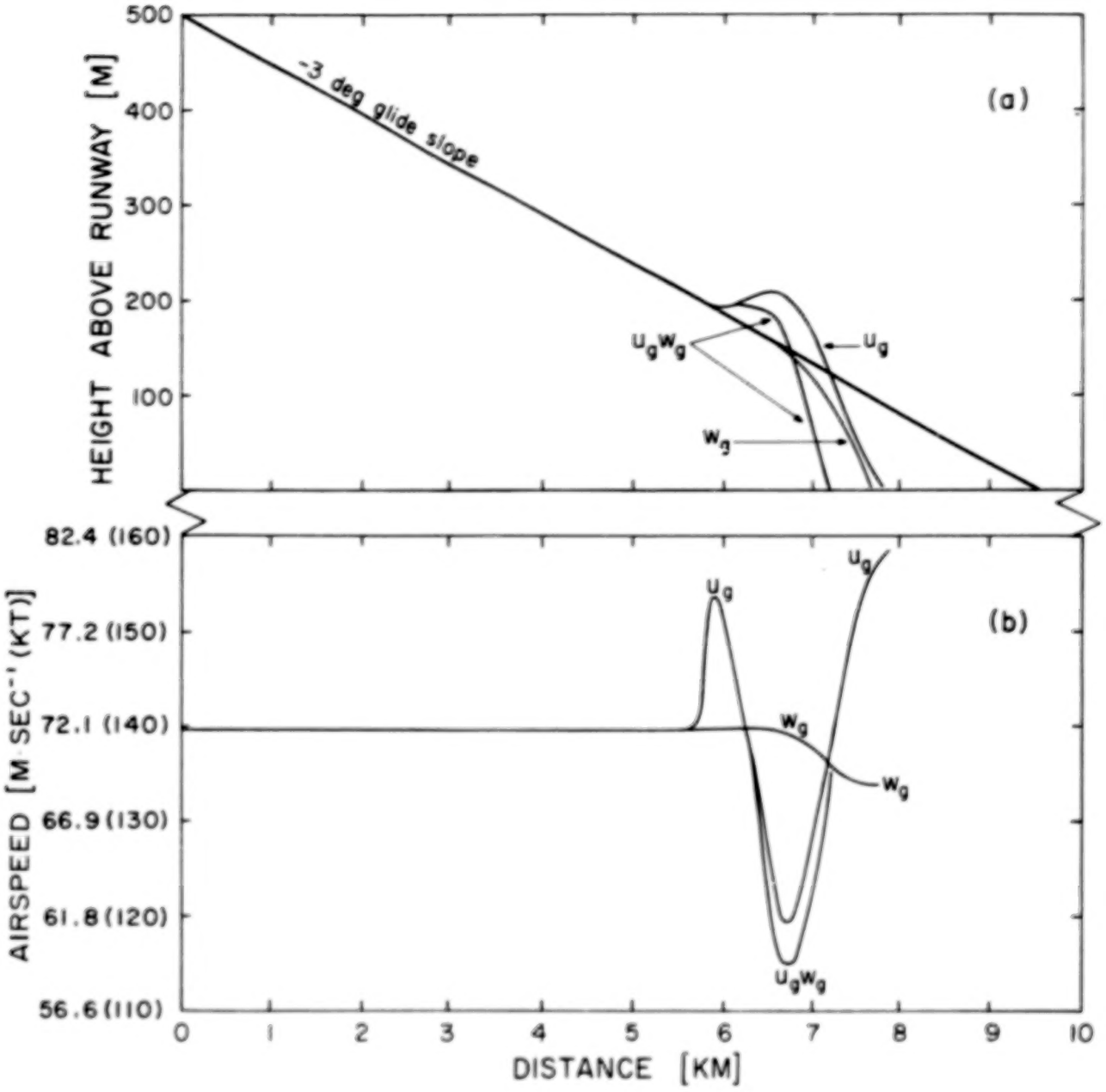

Fig. 16. (a) Model output showing airplane position relative to glide path. Curves are shown for three input environmental winds: longitudinal u_g, vertical w_g, and both u_g and w_g. (b) Model output showing airplane airspeed for three cases in (a). Nominal airspeed is 72.1 m·sec^{-1} (140 kt).

rather than a wave feature. To relate shear to harmonic features, a Fourier analysis of simple shear is performed, suggesting most of the energy density is represented in a sine wave with a 12 sec period. Consequently we can consider the appropriate frequency to be .083 Hz or ω/ω_{ph} = 3.21, as seen in Table 4. From Fig. 4, this frequency clearly represents a small deterioration of approach quality, as seen in the estimated $\Delta u'$ and $\Delta h'$. Notice that the ADP's for ω/ω_{ph} = 3.21 in Fig. 4 are far below those calculated and given in Table 4. This difference may be due to the fact that we are comparing ADP estimates of two highly simplified models; however, the example serves to illustrate the point that the aircraft response to w_g is considerably less than its response to u_g.

Table 4. Approach Deterioration Parameters for JFK simulation (refer to Figs. 15 and 16 for profiles).

Case	$\Delta u'$ $m \cdot sec^{-1}$	$\Delta h'$ (m)	ω (Hz)	ω/ω_{ph}
u_g only	3.5	23.7	.026	1.00
w_g only	0.9	20.4	.083	3.21
u_g, w_g	3.8	22.6		

Returning to the full simulation, note that fluctuations in velocity from 72.1 $m \cdot sec^{-1}$ (140 kt) are large indeed, resulting in a wave-like departure from the nominal value. In terms of the $\Delta u'$ ADP, most of the deterioration occurs because

of the u_g factor. In fact, the calculated values of $\Delta u'$ and $\Delta h'$ agree quite well with the predicted values given in Fig. 4, for the appropriate value of ω/ω_{ph}. We see that the largest values of ADP should be associated with u_g, and the most sensitive indicator is the $\Delta u'$ ADP. Referring again to Fig. 16, we see that the extreme airspeed oscillation associated with u_g bears this out.

The deleterious effect of w_g is present, as seen in the glide slope position plot; however, we contend that the most critical feature is the extreme oscillation in airspeed, due to the aircraft's encounter with high energy at the phugoid frequency.

Inspection of Fig. 4 indicates a large peak in the relationship between w_g and $\Delta h'$, near $\omega = 4.7 \times 10^{-3}$ Hz representing a wave period of 214 sec. We assume that a real pilot easily would be able to overcome such an effect by elevator and thrust corrections, since the time-space scale length is 61% longer than the 133 sec nominal approach period. Use of the fixed-stick mode precluded such a correction here.

The utility of the ARWS function can be seen in the JFK simulation. For example, a $\Delta u'$ of 3.5 $m \cdot sec^{-1}$ requires the product of u_g energy density and transfer function be at least 65 $m^2 \cdot sec^{-2} \cdot Hz^{-1}$ expressed in dB; as shown in Fig. 10. For the Eastern 66 simulation, this value of ARWS presumably represents a critical threshold.

To obtain an estimate of the frequency of occurrence of conditions comparable to those experienced by Eastern 66, the u_g energy density at the phugoid frequency for the 940 near-thunderstorm wind profiles was examined. The cumulative frequency for multiples of the energy density obtained from the wind profile used in the Eastern 66 simulation is shown in Table 5. It can be seen that for these near-thunderstorm conditions, the energy density at the phugoid frequency exceeds the Eastern 66 value for about 8% of the cases and is more than double that value for almost 2% of the cases. This demonstrates that flying conditions as bad as those experienced by Eastern 66 are not extremely rare.

Table 5. Cumulative frequency distribution of energy density at phugoid frequency, as a function of multiples of Eastern 66 computed energy density for u_g at u_{ph}. Tower data values are in parentheses.

Multiples of Eastern 66 Energy Density of 95.24 $m^2 \cdot sec^{-2} \cdot Hz^{-1}$	Cumulative Frequency
0.25	0.373 (0.700)
0.50	0.203 (0.363)
0.75	0.114 (0.225)
1.00	0.078 (0.200)
1.25	0.051 (0.138)
1.50	0.029 (0.125)
1.75	0.022 (0.088)
2.00	0.017 (0.050)

Included in Table 5 are the cumulative frequencies for the 80 tower data cases. It can be seen that 20% of these cases exceed the value of Eastern 66. The results are comparable to the 940 aircraft cases but frequencies are somewhat higher.

In conclusion, we believe that the JFK accident is associated with the airplane's encounter with a horizontal wind containing high energy at the airplane's critical phugoid frequency, which caused a sudden extreme variation in the airspeed. Matters were made worse by the downdraft, but the airplane's response was most seriously affected by u_g variations. We see this explanation as a subtle but important variation from the conclusion of Fujita and Caracena (1977) that a sudden "downburst" drove Eastern 66 into the ground. Their explanation does not consider aircraft response stability as a vital parameter, and leaves the impression that the accident was caused entirely by meteorological events. Our explanation certainly includes meteorological events, including a possible downdraft as an initiating factor, but extends the concept to couple aircraft response factors to the weather. The horizontal wind u_g, perhaps caused by thunderstorm outflow, provides energy at the phugoid frequency, excites a severe horizontal velocity oscillation, leading to loss of control and a possible stall. Furthermore, we must not overlook the reality that an aircraft is likely to encounter

horizontal gustiness more frequently than vertical "downbursts".

At this point it is very interesting to compare Fujita's (1977) analysis of Eastern 66 to our model results seen in Fig. 16. Fig. 17 (from Fujita and Caracena, 1977) shows the flight track of Eastern 66, in a view similar to Fig. 16(a). There is a remarkable similarity between his analysis which requires the downburst explanation, and our u_g curve which includes no w_g component. True, then w_g is added, matters are made slightly worse, but the basis of our alternative explanation is made clear. We must conclude that a consideration of aircraft response theory, as well as environment wind energy, is necessary to fully appreciate the approach hazard.

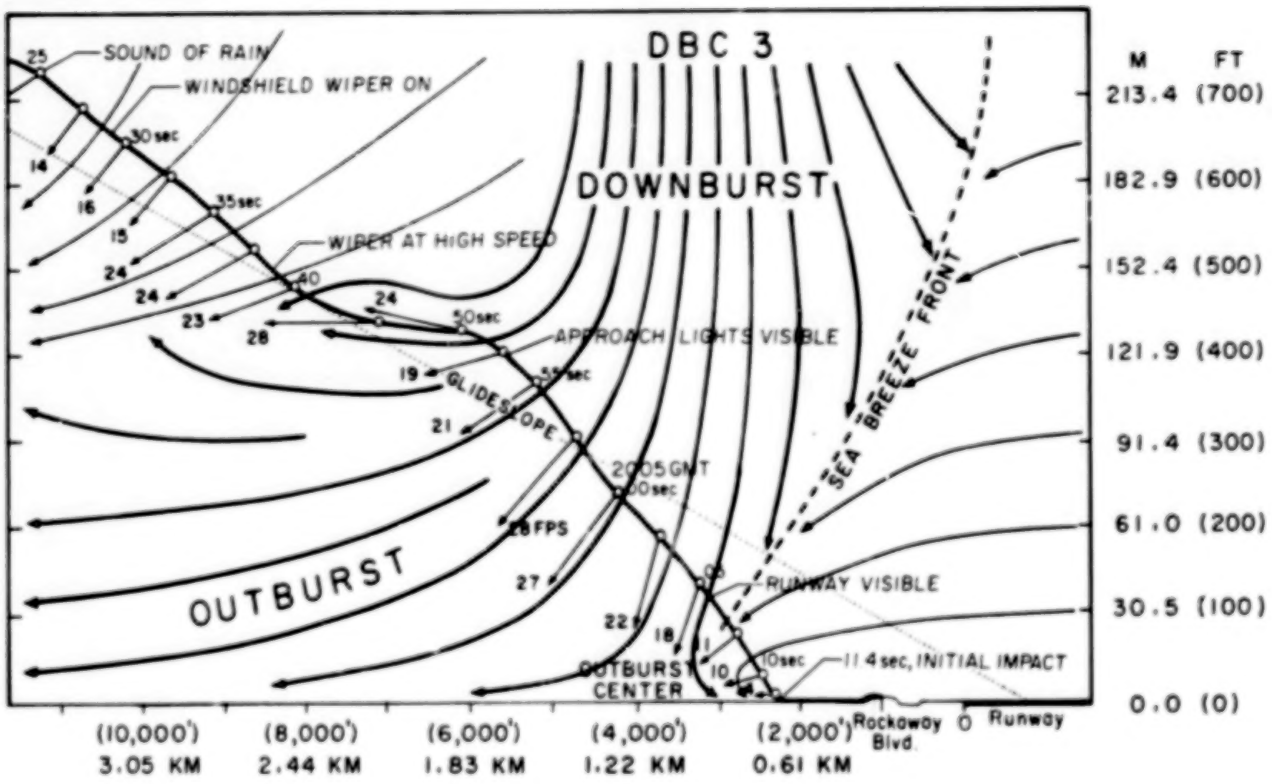

Fig. 17. The path of Eastern 66 on 24 June 1975 in the vertical plane including the glide slope of runway 22-L at JFK (used with permission from Fujita and Caracena, 1977, Fig. 10).

CHAPTER IV

CONCLUSIONS

The work reported herein represents an attempt to combine fundamental aircraft response to the thunderstorm environment wind shear, during an approach-to-landing. Not only have we developed several means of examining the nature of the wind shear, but we have mated it to the basic response characteristics of aircraft. This has resulted in a means to predict the possible deterioration of the approach, for given wind conditions and for a specific aircraft type. We have chosen only one aircraft type for our study, a medium-sized jet transport (Boeing 727 class) as a convenience, and not in any way to single out this airplane, but to represent a typical airliner.

Our examination indicates the presence of wind shear containing energy at our aircraft's resonant or phugoid frequency sufficient to suggest serious deterioration of the approach on about 20% of approximately 1000 cases examined. This deterioration is observed as sudden oscillation in airplane airspeed that can bring the aircraft near stall, or in height oscillations from the glide slope, possibly bringing about a premature impact with the ground short of the runway.

For our aircraft of study, the phugoid frequency is 0.026 Hz, or for an approach speed of 72.1 $m \cdot sec^{-1}$ (140 kt)

a phugoid wavelength of 2.8 km. We are not surprised by our finding that approximately 20% of our cases had phugoid energy sufficient to suggest approach deterioration equal or worse than that encountered by Eastern Flight 66. Such a scale length (near 3 km) would be a typical one in a thunderstorm, for vertical columns (updrafts and downdrafts) occur on such a horizontal length scale. Our study suggests that horizontal variations of the environmental wind along the aircraft's longitudinal axis of motion, are more critical than vertical variations of wind. While these vertical components can deteriorate the approach, it appears that a firm handle on the horizontal component is most important.

Consequently, we believe critical energy at the phugoid frequency is at least not rare in the thunderstorm landing environment, and therefore the national airspace system should take steps to detect and warn approaching aircraft of such problems. It is important to realize that this conclusion about the nature of wind shear is fundamentally a time dependent problem. The existence of atmospheric waves, whose effect on aircraft depends on approach speed as well, requires time variation considerations. Previous wind shear studies have not denied this important point, but have failed to recognize it as critical.

Our work has limitations, to be sure. First of all, it is theoretical in that we simulate flight, rather than consider

a real aircraft. Furthermore, no pilot is considered. Some will suggest that our conclusions are severely limited by this exclusion. We cite our sensitivity studies of elevator input in Chapter II and our Eastern 66 simulation in Chapter III as indicating that phugoidal response problems are still serious when pilot input is included. Finally, we have examined only one type of aircraft. While this of course limits the scope, our objective is not to identify positively whether a specific airplane will in fact crash, but rather to indicate the fundamental nature of the wind shear - aircraft interaction. This interaction exists for all aircraft, but a given wind field may have less serious consequences for some aircraft (our Beech Baron at JFK, for example).

Where do we go from here? We believe a real-time approach deterioration parameter detection system may be feasible. The system would work as follows:

1. A single pulsed Doppler radar would collect radial velocities (from the ground) along intended ILS glide paths to airport runways. These radial components would be essentially identical to u_g components discussed in this work, after making a frozen turbulence hypothesis. Remember, our work has indicated the u_g component should be a good "trouble" predictor.
2. The u_g data would be collected at discrete distances

along the glide path, then converted to the time series input form by knowing the aircraft approach speed. This u_g as a function of time would be fed into the simulation model, which would be adjusted for a type of aircraft.

3. The model output would predict an ARWS parameter which could be used by the ATC controller and/or pilot to decide whether severe conditions exist along the intended approach.

The advantages of this system could be many. It would not require an actual and possible dangerous approach to be utilized. A quantitative estimate of ADP would be available at all times. The ADP would be mated to aircraft type (although we do not expect the system to be used to let some aircraft to land, while forcing others to go around).

The authors are in the process of testing the feasibility of such a system, with the hopes that an operational system could be implemented in the early 1980's.

REFERENCES

Frost, W., and B. Crosby, 1978: Investigations of simulated aircraft flight through thunderstorm outflows. NASA Contractor Report 3052, 110 pp.

_____, and K. R. Reddy, 1978: Investigation of aircraft landing in variable wind fields. NASA Contractor Report 3073, 84 pp.

_____, D. W. Camp, and S. T. Wang, 1978: Wind shear modeling for aircraft hazard definition. FAA Report No. FFA-RD-78-3, 240 pp.

Fujita, T. T., and H. R. Byers, 1977: Spearhead echo and downburst in the crash of an airliner. Mon. Wea. Rev., 102, 129-146.

_____, and F. Caracena, 1977: An analysis of three weather-related aircraft accidents. Bull. Amer. Meteor. Soc., 11, 1164-1181.

Goerss, J. S., and A. J. Koscielny, 1977: Monte Carlo estimation of confidence limits for maximum entropy spectra. Preprints 5th Conf. Prob. and Stat. in the Atmos. Sci., Las Vegas, Amer. Meteor. Soc., 297-302.

McCarthy, J., and E. F. Blick, 1976: Aircraft response to boundary layer turbulence and wind shear associated with cold-air-outflow from a severe thunderstorm. Preprints 7th Conf. Aerospace and Aeronautical Meteor. and Symposium on Remote Sensing from Satellites, Melbourne, Fl., Amer. Meteor. Soc., 62-69.

_____, _____, and R. R. Bensch, 1978b: A spectral analysis of thunderstorm turbulence and jet transport landing performance. Conf. Atmos. Environment of Aerospace Systems and Applied Meteor., New York, Amer. Meteor. Soc.

_____, _____, _____, and N. R. Sarabudla, 1978a: Effect of wind turbulence and shear on landing performance of jet transports. Preprints 16th AIAA Aerospace Sciences Meeting, Huntsville, Al., Amer. Institute of Aeronautics and Astronautics.

McRuer, D., I. Ashkenas, and D. Graham, 1973: Aircraft Dynamics and Automatic Control. Princeton Univ. Press, 313 pp.

National Transportation Safety Board, 1974: Accident Report - Delta Airlines, Inc. Douglas DC-9-32, Chattanooga Municipal Airport, Chattanooga, Tennessee, November 27, 1973; NTSB-AAR-74-13, Washington, D.C.

_____, 1976a: Accident Report - Eastern Airlines, Inc. Boeing 727-225, John F. Kennedy Airport, Jamaica, New York, June 24, 1975, NTSB-AAR-76-8 Washington, D.C., 47 pp.

_____, 1976b: Accident Report - Continental Airlines, Inc. Boeing 727-224, Stapelton International Airport, Denver, Colorado, August 7, 1975; NTSB-AAR-76-14, Washington, D.C.

Roskam, J., 1972: Flight Dynamics of Rigid and Elastic Airplanes, Part 1. Pub. by author, 519 Boulder, Lawrence, Ks., 619 pp.

Ulrych, T. J., and T. N. Bishop, 1975: Maximum entropy spectral analysis and autoregressive decomposition. Rev. Geophysics and Space Physics, 13, 183-200.

TECHNICAL REPORT STANDARD TITLE PAGE

1. REPORT NO.	2. GOVERNMENT ACCESSION NO.	3. RECIPIENT'S CATALOG NO.
NASA CR-3207		

4. TITLE AND SUBTITLE	5. REPORT DATE
Jet Transport Performance in Thunderstorm Wind Shear Conditions	December 1979
	6. PERFORMING ORGANIZATION CODE
7. AUTHOR(S)	8. PERFORMING ORGANIZATION REPORT #
John McCarthy, Edward F. Blick, and Randall R. Bensch	
9. PERFORMING ORGANIZATION NAME AND ADDRESS	10. WORK UNIT NO.
The University of Oklahoma Norman, Oklahoma	M-290
	11. CONTRACT OR GRANT NO.
	NAS8-31377
	13. TYPE OF REPORT & PERIOD COVERED
12. SPONSORING AGENCY NAME AND ADDRESS	Contractor
National Aeronautics and Space Administration Washington, D. C. 20546	14. SPONSORING AGENCY CODE

15. SUPPLEMENTARY NOTES

Prepared under the technical monitorship of the Atmospheric Sciences Division, Space Sciences Laboratory, NASA Marshall Space Flight Center

16. ABSTRACT

Several hours of three-dimensional wind data were collected in the thunderstorm approach-to-landing environment, using an instrumented NCAR Queen Air airplane. These data were used as input to a numerical simulation of aircraft response, concentrating on fixed-stick assumptions, while the aircraft simulated an ILS approach. Output included airspeed, vertical displacement, pitch angle, and a special approach deterioration parameter. Theory and the results of approximately 1000 simulations indicated that about 20 percent of the cases contained serious wind shear conditions capable of causing a critical deterioration of the approach. In particular, the presence of high energy at the airplane's phugoid frequency was found to have a deleterious effect on approach quality. Oscillations of the horizontal wind at the phugoid frequency were found to have a more serious effect than vertical wind. A simulation of Eastern Flight 66, which crashed at JFK in 1975, served to illustrate the points of the research. A concept of a real-time wind shear detector was outlined, utilizing these results.

17. KEY WORDS	18. DISTRIBUTION STATEMENT
Thunderstorm Wind shear Phugoid frequency Aviation safety Wind spectra Flight simulation	Category 47

19. SECURITY CLASSIF. (of this report)	20. SECURITY CLASSIF. (of this page)	21. NO. OF PAGES	22. PRICE
Unclassified	Unclassified	61	

MSFC - Form 3293 (Rev. December 1972)

For sale by National Technical Information Service, Springfield, Virginia 22161

NASA-Langley, 1979

END

6-11-81

90 %

50 %